

1 **Elemental Ratio Measurements of Organic Compounds**
2 **using Aerosol Mass Spectrometry: Characterization,**
3 **Improved Calibration, and Implications**

4
5 **Canagaratna, M.R.¹, Jimenez, J. L.², Kroll, J. H.^{3,4}, Chen, Q.³, Kessler, S. H.⁴**
6 **, Massoli, P.¹ Hildebrandt Ruiz, L.⁵, Fortner, E.¹, Williams, L. R.¹, Wilson, K.**
7 **R.⁶, Surratt, J. D.⁷, Donahue, N. M.⁸, Jayne, J.T.¹, and Worsnop, D.R.¹**

8
9 [1]{Aerodyne Research, Inc. Billerica, MA, USA }

10 [2]{Department of Chemistry and Biochemistry, and Cooperative Institute for Research
11 in the Environmental Sciences (CIRES), University of Colorado, Boulder, CO, USA }

12 [3]{Department of Civil and Environmental Engineering, Massachusetts Institute of
13 Technology, Cambridge, MA, USA }

14 [4]{Department of Chemical Engineering, Massachusetts Institute of Technology,
15 Cambridge, MA, USA }

16 [5]{McKetta Department of Chemical Engineering, and Center for Energy and
17 Environmental Resources, The University of Texas at Austin, Austin, TX, USA }

18 [6]{Lawrence Berkeley National Lab, Berkeley, CA, USA }

19 [7]{Department of Environmental Science and Engineering, University of North
20 Carolina, Chapel Hill, NC, USA }

21 [8]{Center for Atmospheric Particle Studies, Carnegie Mellon University, Pittsburgh,
22 PA, USA }

23 Correspondence to: M. R. Canagaratna (mrcana@aerodyne.com)

24 **Abstract**

25 Elemental compositions of organic aerosol (OA) particles provide useful constraints on
26 OA sources, chemical evolution, and effects. The Aerodyne high-resolution time-of-
27 flight aerosol mass spectrometer (HR-ToF-AMS) is widely used to measure OA
28 elemental composition. This study evaluates AMS measurements of atomic oxygen-to-
29 carbon (O:C), hydrogen-to-carbon (H:C), organic mass-to-organic carbon (OM:OC), and

1 carbon oxidation state ($\overline{\text{OS}}_{\text{C}}$) for a vastly expanded laboratory dataset of multifunctional
2 oxidized OA standards. For the expanded standard dataset, the method introduced by
3 Aiken et al. (2008), which uses experimentally measured ion intensities at all ions to
4 determine elemental ratios (referred to here as "Aiken-Explicit"), reproduces known O:C
5 and H:C ratio values within 20% (average absolute value of relative errors) and 12%
6 respectively. The more commonly used method, which uses empirically estimated H_2O^+
7 and CO^+ ion intensities to avoid gas phase air interferences at these ions (referred to here
8 as "Aiken-Ambient"), reproduces O:C and H:C of multifunctional oxidized species
9 within 28% and 14% of known values. The values from the latter method are
10 systematically biased low, however, with larger biases observed for alcohols and simple
11 diacids. A detailed examination of the H_2O^+ , CO^+ , and CO_2^+ fragments in the high-
12 resolution mass spectra of the standard compounds indicates that the Aiken-Ambient
13 method underestimates the CO^+ and especially H_2O^+ produced from many oxidized
14 species. Combined AMS-vacuum ultraviolet (VUV) ionization measurements indicate
15 that these ions are produced by dehydration and decarboxylation on the AMS vaporizer
16 (usually operated at 600 °C). Thermal decomposition is observed to be efficient at
17 vaporizer temperatures down to 200 °C. These results are used together to develop an
18 "Improved-Ambient" elemental analysis method for AMS spectra measured in air. The
19 Improved-Ambient method uses specific ion fragments as markers to correct for
20 molecular functionality-dependent systematic biases and reproduces known O:C (H:C)
21 ratios of individual oxidized standards within 28% (13%) of the known molecular
22 values. The error in Improved-Ambient O:C (H:C) values is smaller for theoretical
23 standard mixtures of the oxidized organic standards, which are more representative of
24 the complex mix of species present in ambient OA. For ambient OA, the Improved-
25 Ambient method produces O:C (H:C) values that are 27% (11%) larger than previously
26 published Aiken-Ambient values; a corresponding increase of 9% is observed for
27 OM:OC values. These results imply that ambient OA has a higher relative oxygen
28 content than previously estimated. The $\overline{\text{OS}}_{\text{C}}$ values calculated for ambient OA by the
29 two methods agree well, however (average relative difference of 0.06 $\overline{\text{OS}}_{\text{C}}$ units). This
30 indicates that $\overline{\text{OS}}_{\text{C}}$ is a more robust metric of oxidation than O:C, likely since $\overline{\text{OS}}_{\text{C}}$ is not
31 affected by hydration or dehydration, either in the atmosphere or during analysis.

1 1 Introduction

2 Organic aerosols (OA) account for a substantial fraction of ambient submicron aerosol
3 mass in urban and rural/remote environments, with important impacts ranging from
4 human health to climate forcing (IPCC, 2007;Pope and Dockery, 2006) . In recent years
5 the Aerodyne Aerosol Mass Spectrometers (AMS; (Canagaratna et al., 2007)) have seen
6 wide use for characterizing the composition, the elemental ratios (H:C, O:C, N:C, S:C,
7 OM:OC) (Aiken et al., 2007;Aiken et al., 2008) and the approximate carbon oxidation
8 state ($\overline{OS}_C \approx 2 \times O:C - H:C$) of OA (Kroll et al., 2011). This information provides key
9 constraints for understanding aerosol sources, processes, impacts, and fate, and for
10 experimentally constraining and developing predictive aerosol models on local, regional,
11 and global scales.

12 Organic aerosol elemental ratios can be measured with a number of analytical techniques
13 besides the AMS. These include combustion analysis (O'Brien et al., 1975;Krivacsy et
14 al., 2001;Kiss et al., 2002), electrospray ionization coupled to ultrahigh-resolution mass
15 spectrometry with (ESI) (Nguyen and Schug, 2008;Altieri et al., 2009;Bateman et al.,
16 2009;Kroll et al., 2011;Mazzoleni et al., 2010), nuclear magnetic resonance (NMR)
17 spectroscopy (S. Fuzzi et al., 2001), Fourier transform infrared spectroscopy (FTIR)
18 (Gilardoni et al., 2009;Mysak et al., 2011), and X-ray photoelectron spectroscopy (XPS)
19 (Mysak et al., 2011). Gas chromatography-mass spectrometry (GC-MS) (Williams et
20 al., 2006) and Chemical ionization mass spectrometry (CIMS) with aerosol collection
21 interface have also recently been coupled to a high-resolution time-of-flight mass
22 spectrometer to allow for determination of elemental ratios (i.e. O:C and H:C) of organic
23 aerosols (Lopez-Hilfiker et al., 2014; Yatavelli and Thornton, 2010; Williams et al.
24 2014). Each of these techniques has its own strengths and weaknesses. AMS
25 measurements of bulk aerosol elemental composition are obtained directly from the
26 average elemental compositions of the individual fragment ions observed in high-
27 resolution AMS spectra. One strength of the AMS approach is that it offers the capability
28 for online, sensitive detection of aerosol elemental composition. A weakness is its use of
29 empirical corrections that can affect the accuracy of the calculated elemental ratios. This

1 manuscript evaluates the accuracy of the AMS elemental analysis approach over a wider
2 range of OA species than has been studied before.

3 In the AMS, aerosol particles are focused into a beam in a high-vacuum chamber and
4 typically flash-vaporized on a tungsten vaporizer at a temperature of 600°C before
5 constituents are detected with electron ionization (EI) mass spectrometry. Thus, the
6 elemental composition obtained from AMS mass spectra can be potentially biased by two
7 sources: vaporization and ion fragmentation. Organic molecules, particularly oxidized
8 organic species comprising oxidized organic aerosol (OOA), can decompose during the
9 AMS vaporization process to form stable molecules with elemental compositions that
10 differ from the original parent molecule. Carboxylic acids and alcohols, for example, are
11 known to undergo thermally induced dehydration and decarboxylation as follows
12 (Moldoveanu, 2009):



15 The decomposition products are all ionized and detected by the AMS. The loss of neutral
16 CO₂, CO, and H₂O from the parent carboxylic acid and alcohol molecules results in the
17 formation of organic ions in EI (R⁺ and their fragments) that differ significantly from
18 their parents in chemical identity and elemental composition. The accuracy with which
19 the parent elemental ratios are calculated from AMS measurements will depend on the
20 accuracy with which the C, H, and O masses in all of the decomposition fragments are
21 measured or accounted for. Mass spectral interferences from gas and particle species
22 further complicate accurate determinations of H₂O⁺ and CO⁺ intensities for OA sampled
23 in air (Aiken et al., 2008).

24 Previous work by Aiken et al. (2008;2007) showed that O:C and H:C ratios of laboratory
25 standard molecules can be estimated to within 31% and 10% (average absolute value of
26 the relative error, respectively) with the AMS. The "Aiken-Explicit" (A-E) method
27 averages the elemental composition of all measured fragment ions observed in high-
28 resolution mass spectra and uses H:C and O:C calibration factors derived from laboratory
29 measurements of standard organic molecules. The calibration factors account for
30 differences between the elemental compositions of the detected fragment ions and their

1 parent molecules, e.g. due to the tendency of more electronegative fragments with high O
2 content to end up as neutrals rather than as positive ions during the ion fragmentation
3 process. The "Aiken-Ambient" (A-A) method is similar; however, it uses empirically
4 estimated H_2O^+ and CO^+ intensities for OA sampled in air. The Aiken-Ambient method
5 is used widely for elemental analysis of ambient and chamber OA because the intensities
6 of H_2O^+ and CO^+ originating from OA are difficult to separate from those originating
7 from other background species in air.

8 In this study we extend the Aiken et al. (2007,2008) elemental analysis calibrations to a
9 wider range of OA species. The Aiken et al. (2007,2008) calibration dataset used
10 consisted of reduced primary OA (POA)-like organic species and a few OOA surrogates
11 such as dicarboxylic, fulvic, and amino acids. The species chosen for the present study
12 contain multi-functional oxygenated moieties and have high O:C values that are more
13 representative of ambient OOA species. We investigate the extent to which thermal
14 decomposition of these species (cf. Reactions R1 and R2) bias elemental ratio
15 measurements obtained with the AMS. AMS data from the laboratory standard
16 molecules are used to re-evaluate the Aiken-Explicit and Aiken-Ambient methods for
17 calculating elemental ratios. An "Improved-Ambient" (I-A) method (for AMS
18 measurements performed in air) is determined as part of this study; the changes caused by
19 application of the Improved-Ambient method to previously published ambient and
20 chamber data are discussed. Empirical relationships used to determine O:C and H:C
21 ratios from unit mass resolution AMS spectra are also updated to reflect the improved
22 calibrations.

24 **2 Methods**

25 **2.1 Aerosol standards**

26 A list of the aerosol standards used in this study is given in Table 1. This list includes
27 alcohols, diacids, polyacids, esters, and other species with multiple functionalities such as
28 keto and hydroxy acids. All of the standards were purchased from Sigma-Aldrich (purity
29 ranges > 96%) except for three synthesized standards including a racemic mixture of δ -

1 isoprene epoxydiol (IEPOX) diastereomers known to be intermediates in isoprene
2 oxidation chemistry, as well as known isoprene-derived SOA constituents *cis*- and *trans*-
3 3-methyl-3,4-dihydroxytetrahydrofurans (Lin et al., 2012;Zhang et al., 2012)

4 Aerosol particles were generated by dissolving small amounts of each standard in
5 about 100 mL of distilled water, followed by atomization. The standards were atomized
6 with argon carrier gas instead if nitrogen, since gaseous nitrogen in air produces a very
7 large peak at m/z 28 that make CO^+ aerosol signals very difficult to separate and quantify
8 (even at high-resolution). Detection of CO^+ is of great interest since this ion is a likely
9 thermal decomposition fragment of acids and potentially other species in OOA. The
10 resulting polydisperse aerosol was then dried (with two silica gel diffusion dryers in
11 series) in order to remove any remaining water from the atomization process and sampled
12 directly into the AMS. The humidity of the flow after drying was spot checked for
13 several experiments and was found to reproducibly be $< 4\%$. Any H_2O that was not
14 removed from the particles after exposure to these conditions is likely to have been
15 further lost by evaporation when the particles encounter the 2 mbar sampling conditions
16 of the AMS aerodynamic lens. Taken together it is likely that the aerosol H_2O was
17 negligible in these experiments and uncertainties due to the presence of aerosol H_2O
18 should have been small. The atomization setup was thoroughly cleaned between
19 standards and blank water runs were carried out in between standards to ensure that
20 cleaning between each set of standards was successful.

21 **2.2 AMS operation and data analysis**

22 The HR-ToF-AMS instrument and its data analysis procedures have been described in
23 detail in previous publications (Canagaratna et al., 2007;DeCarlo et al., 2006). The HR-
24 ToF-AMS can be usually operated in two ion optical modes (V or W) with differing
25 spectral resolutions. For these experiments the AMS was operated in the more sensitive
26 V-mode. The resolution of this mode (resolving power of ~ 3000) was high enough to
27 resolve the key isobaric fragments observed from the standards studied here. The higher
28 signal levels observed in the V-mode also allowed for the use of low-concentration
29 samples in the atomizer, thereby minimizing cross-contamination between standards and
30 avoiding signal saturation of the AMS detector or acquisition card. High-resolution ions

1 up to the molecular weight of each standard were fitted in order to account for all of its
2 ion fragments. The AMS data analysis software packages SQUIRREL (version 1.51H) and
3 PIKA (version 1.10H) were used for the analysis of the high-resolution mass spectra. This
4 software allows for ready calculation of elemental ratios from both A-A and A-E
5 methods. The A-A calculation uses the default organic fragmentation wave proposed by
6 Aiken et al. (2008) and the A-E method uses a copy of the default organic fragmentation
7 wave in which the entries for m/z 28,18,17, and 16 are replaced to use measured ion
8 intensities rather than estimated values. The I-A elemental ratios discussed below use A-
9 A values and marker ion relative intensities calculated from normalized organic mass
10 spectra output by the PIKA software.

11 Data collection occurred over several months and some standards were repeatedly
12 measured at different points in time with the same instrument. Supplementary Fig. 1a
13 shows the standard deviations in O:C and H:C values (calculated using Aiken-Ambient
14 method) obtained during these measurements. As can be seen, for most standards O:C
15 and H:C values obtained on a given instrument are reproducible to <5% and <3%
16 respectively. Supplementary Fig(s). 1b and 1c compare O:C and H:C values obtained for
17 different standards on three AMS instruments. The values compare well across
18 instruments (O:C within 4%, H:C within 7%).

19 For most of the experiments the AMS vaporizer was operated at a power corresponding
20 to 600°C. The thermocouple readout from the vaporizer is sensitive to its exact
21 placement on the vaporizer and can sometimes differ from instrument to instrument or
22 vary with instrument use. Thus, the measurements were standardized by varying the
23 vaporizer power to minimize the width of a monodisperse 350 nm NaNO₃ aerosol size
24 distribution measured by the AMS. The time-of-flight traces of the NO⁺ ion (m/z 30)
25 from NaNO₃ were monitored as a function of vaporizer ion current. The optimum AMS
26 vaporizer current is obtained by subtracting 0.1 amps from the vaporizer current at which
27 the narrowest NO⁺ ion time-of-flight traces are observed from NaNO₃. Typically this
28 optimum AMS vaporizer current is near 1 amp. In most cases the thermocouple readout
29 at the optimum heater power setting read temperatures in the range 590-600°C, indicating
30 that the thermocouples in these instruments were providing a reasonably accurate
31 measure of the actual heater temperature. In addition to the standard 600°C operation, a

1 few experiments were also performed at 200°C (about the lowest temperature at which
2 the AMS vaporizer can be operated continuously) in order to investigate how the amount
3 of thermal decomposition and ion fragmentation changed with temperature. In both of
4 these cases the typical vaporization timescale for particles was measured to be on the
5 order of one hundred microseconds.

6 **2.3 VUV ionization**

7 Northway et al. (2007) described the adaptation of an HR-ToF-AMS to the vacuum
8 ultraviolet (VUV) beam at the Advanced Light Source (Lawrence Berkeley Laboratory).
9 We performed a similar adaptation in this study and generated and analyzed selected
10 standards (see Table 1) using the same procedures discussed above. Previous work has
11 shown that, compared to 70 eV EI-AMS spectra, VUV-AMS spectra are typically less
12 complex, with reduced ion fragmentation and increased molecular ion intensity
13 (Canagaratna et al., 2007;Northway et al., 2007). Molecular ions observed in VUV-AMS
14 spectra of unoxidized and slightly oxidized squalane have been successfully used to
15 obtain chemical and mechanistic insight into the squalane oxidation reaction (Smith et al.,
16 2009). Moreover, the tunability of the VUV light can be used to investigate the chemical
17 identity of species by measuring their threshold ionization energy (Leone et al., 2010).
18 The threshold ionization energy of most organic molecules is 10.5 eV and that of H₂O,
19 CO₂, and CO molecules is 12.62 eV, 13.77,eV, and 14.01 eV respectively (NIST
20 Chemistry WebBook: <http://webbook.nist.gov/chemistry/>). Thus, in this experiment the
21 8eV to 14.5 eV VUV range was used.

22 **2.4 Elemental analysis (EA) methods**

23 The procedure for obtaining elemental ratios (O:C, H:C) from AMS spectra was first
24 developed by Aiken et al (2007,2008). The atomic O:C and H:C ratios are obtained in
25 terms of the relative mass concentrations of O (M_O) and C (M_C) and H (M_H) as follows:

$$26 \quad \text{O:C} = \alpha_{\text{O:C}} \times (M_O/M_C) \times (MW_C/MW_O) \quad (1)$$

$$27 \quad \text{H:C} = \alpha_{\text{H:C}} \times (M_H/M_C) \times (MW_C/MW_H) \quad (2)$$

28 MW_C , MW_O and MW_H are the atomic weights of C, O, and H respectively. Since AMS
29 ion intensities are proportional to the mass of the original molecules present (Jimenez et

1 al., 2003), M_C , M_O , and M_H are obtained as a sum of the appropriate ion intensities across
2 the complete organic spectrum (including H_2O^+ , CO^+ , and CO_2^+) as follows:

$$3 \quad M_C = \sum_{j=m/z_{min}}^{m/z_{max}} I_j F_C \quad (3)$$

$$4 \quad M_O = \sum_{j=m/z_{min}}^{m/z_{max}} I_j F_O \quad (4)$$

$$5 \quad M_H = \sum_{j=m/z_{min}}^{m/z_{max}} I_j F_H \quad (5)$$

6 where I_j is the ion intensity of the j^{th} ion in the spectrum and F_C , F_O , F_H are the relative
7 carbon, oxygen, and hydrogen mass fractions for that ion. Calibration parameters ($\alpha_{O:C}$
8 and $\alpha_{H:C}$) account for preferential losses of some atoms to neutral rather than ion
9 fragments during the fragmentation processes. The tendency of hydrocarbon fragments
10 to form positive ions more readily than those containing the more electronegative O
11 atom, for example, can result in such a detection bias. Aiken et al. (2008) obtained slopes
12 of 0.75 and 0.91 (i.e. $\alpha_{O:C} = 1/0.75$ and $\alpha_{H:C} = 1/0.91$), respectively, by comparing
13 measured and known O:C and H:C values for a range of organic standards according to
14 Eqs. (1) and (2).

15 In AMS elemental analysis, Eqs. (1) and (2) are applied in two different ways which we
16 refer to here as the Aiken-Explicit and Aiken-Ambient methods (Aiken et al., 2008). The
17 Aiken-Explicit method is used when organic signals at H_2O^+ and CO^+ can be directly
18 measured. Laboratory measurements performed in an atmosphere of dry argon, for
19 example, do not contain the interfering H_2O or N_2 species and allow for direct
20 measurement of the organic signals at CO^+ and H_2O^+ . The organic signals at CO^+ have
21 also been obtained under ambient conditions from AMS size distributions and by
22 monitoring changes in the m/z 28 intensities (Zhang et al., 2005; Takegawa et al., 2007).

1 Calibrations have also been carried out in laboratory chamber experiments under
2 controlled relative humidity to determine the interference signals and obtain the organic
3 signals at CO^+ and H_2O^+ by subtraction (Chen et al., 2011; Nakao et al., 2013).

4 The Aiken-Ambient method is used for measurements performed in air where the
5 interferences from gaseous N_2 and H_2O are difficult to estimate. Since most field
6 measurements and laboratory chamber measurements are performed under the latter
7 conditions, this method has in practice been the most widely used method of obtaining
8 elemental ratios from AMS measurements. In the Aiken-Ambient method the organic
9 H_2O^+ and CO^+ intensities used in Eqs. (3)-(5) are empirically estimated rather than
10 directly measured. The $\text{H}_2\text{O}^+/\text{CO}_2^+$ and $\text{CO}^+/\text{CO}_2^+$ ratios recommended by Aiken et al.
11 (2008) were empirically estimated from limited ambient OA measurements available at
12 the time to be 0.225 and 1 respectively. The $\text{CO}^+/\text{CO}_2^+$ ratio was determined from AMS
13 size distribution measurements where the gas-phase signal from N_2 can be separated from
14 the particle phase CO signal intensities (Zhang et al., 2005; Takegawa et al., 2007). The
15 $\text{H}_2\text{O}^+/\text{CO}_2^+$ mass ratio was empirically estimated to conserve OA mass concentrations
16 that resulted from the new $\text{CO}^+/\text{CO}_2^+$ ratio. This $\text{H}_2\text{O}^+/\text{CO}_2^+$ empirical mass ratio
17 corresponds to a raw ion signal ratio of either 0.225, assuming H_2O^+ and CO_2^+ were each
18 formed with a relative ionization efficiency (RIE) of 1.4 or 0.321, using a recently-
19 determined RIE of 2.0 for the formation of H_2O^+ (Mensah et al., 2011).

21 **3 Results and Discussion**

22 **3.1 Evaluation of Aiken-Explicit and Aiken-Ambient Methods**

23 We evaluated the performance of both Aiken-Explicit and Aiken-Ambient methods over
24 a large range of species, including those with higher O:C and more multifunctional
25 moieties than originally studied by Aiken et al. (2008). Panels a and b in Fig. 1 show
26 elemental ratios obtained with the Aiken-Explicit method for the laboratory standards
27 studied here. The Aiken-Explicit method results reproduce actual O:C and H:C ratios for
28 all the standard molecules with an average absolute value of the relative error (referred to
29 as "error" in the rest of this manuscript) of 20% and 12% respectively. This is consistent

1 with the accuracies reported by Aiken et al. (2008) and confirms that the Aiken-Explicit
2 method can be used for a wide range of OA species.

3 Figures 1c and 1d show Aiken-Ambient results for the laboratory standards. In general
4 the Aiken-Ambient O:C values are biased low for all the standards and observed errors
5 are dependent on the functional groups contained in the different standard molecules.
6 The Aiken-Ambient values for multifunctional standard molecules are biased low by
7 28% and those for diacids and alcohols are biased low by 46%. The error in Aiken-
8 Ambient H:C values for all standards is smaller, but alcohols and diacids are still biased
9 low compared to multifunctional species.

10 **3.2 Measurements of H_2O^+ , CO^+ and CO_2^+ signal intensities with Electron** 11 **Ionization (EI)**

12 The only difference between the Aiken-Explicit and Aiken-Ambient methods is the
13 measured vs. estimated H_2O^+ and CO^+ ion intensities. Since these ion intensities are
14 estimated based on assumed H_2O^+ and CO^+ ratios to CO_2^+ , we investigate trends in the
15 relative signal intensities of these 3 key ions in the observed standard mass spectra.
16 Figure 2 shows the fractional AMS ion intensities (relative to the total ion signal for each
17 standard) measured for these key thermal decomposition products in the spectra of the
18 different laboratory standards. The standards are separated according to functionality,
19 and they are arranged according to increasing molecular O:C. Measurements of the same
20 standard on different instruments are shown as separate bars on the graph. The general
21 agreement between different instruments supports the reproducibility and transferability
22 of the results obtained here to other AMS instruments. The relative intensities of the
23 three ions vary according to specific differences in the decomposition mechanisms
24 including those shown in Reactions (R1) and (R2) above. Spectra from carboxylic acids,
25 esters, polyacids, and multifunctional acids have higher $f_{\text{CO}_2^+}$ (defined as the intensity of
26 CO_2^+ divided by the total ion intensity) and f_{CO^+} than alcohols, indicative of
27 decarboxylation. On the other hand, spectra from alcohols have negligible $f_{\text{CO}_2^+}$ and
28 significant $f_{\text{H}_2\text{O}^+}$, indicative of dehydration (Reaction R2).

1 Figure 3a shows the f_{CO^+} vs. $f_{\text{CO}_2^+}$ scatter plot for all the standards in this study. For
2 most multifunctional systems, the $f_{\text{CO}^+}/f_{\text{CO}_2^+}$ ratio is relatively consistent with the
3 assumed value of 1 from Aiken et al. (2008). The measured $f_{\text{CO}^+}/f_{\text{CO}_2^+}$ ratios for alcohols
4 and most diacids are ≥ 2 which likely contributes to the additional underestimation in
5 O:C that is observed for these species with the Aiken-Ambient method. These
6 measurements are generally consistent with previous studies that have shown that most
7 laboratory SOA (thought to contain a mixture of multifunctional species) yield $f_{\text{CO}^+}/$
8 $f_{\text{CO}_2^+}$ values around 1 (Chhabra et al., 2010; Chen et al., 2011) with exceptions of SOA
9 produced by isoprene photooxidation (2.63; Chen et al., (2011)) and glyoxal uptake under
10 dark, humid conditions (5.0; Chhabra et al. (2010)), both of which contain products that
11 are rich in hydroxyl functional groups but poor in carboxyl groups (Hastings et al.,
12 2005; Lin et al., 2012). Ambient estimates are also in the similar range of 0.9-1.3
13 (Takegawa et al., 2007; Zhang et al., 2005). The $f_{\text{CO}^+}/f_{\text{CO}_2^+}$ ratios discussed above are
14 summarized in Table 2.

15 The relationship between $f_{\text{H}_2\text{O}^+}$ and $f_{\text{CO}_2^+}$ for the standard spectra are shown in Fig. 3b and
16 Table 2. The observed signal intensity ratios in the spectra are larger than those
17 calculated from the empirical mass ratios of Aiken et al. (2008). The measured $f_{\text{H}_2\text{O}^+}/$
18 $f_{\text{CO}_2^+}$ ratio of multifunctional species varies from near 0 to over 2, and many diacids are
19 between 1 and 2 (although some are substantially lower than 1). Polyols and alcohol
20 spectra have even higher ratios, mainly due to their lack of CO_2^+ . As shown in Table 2,
21 similar departures from the assumed $f_{\text{H}_2\text{O}^+}/f_{\text{CO}_2^+}$ ratios were originally observed for
22 chamber SOA by Chen et al. (2011) (0.84-3.91) and more recently by Nakao et al. (2013)
23 (0.33-1.23). We note that in mixed ambient aerosols the $f_{\text{H}_2\text{O}^+}/f_{\text{CO}_2^+}$ ratios would be
24 moderated by the presence of species other than alcohols. However, high values for this
25 ratio (1.0) were also reported for ambient measurements from Whistler mountain (Sun et
26 al., 2009). It is clear from Fig. 3 that the biases in the elemental ratios obtained with the
27 Aiken-Ambient method are due to underestimations of the assumed $f_{\text{H}_2\text{O}^+}/f_{\text{CO}_2^+}$ and $f_{\text{CO}^+}/$
28 $f_{\text{CO}_2^+}$ values. The H_2O^+ and CO^+ intensities observed for alcohols, in particular, are

1 severely underestimated in the current assumptions since the estimates are tied to CO_2^+ ,
2 an ion that is not produced in any significant intensity in spectra of species that do not
3 contain $-\text{C}(\text{O})\text{OR}$ moieties (e.g. alcohols).

4 In the Aiken-Ambient method the intensities of the OH^+ and O^+ fragments of H_2O^+ are
5 estimated according to the ratios measured for gas-phase H_2O . Figure S4 in the
6 supplement shows the scatter plots of measured f_{OH^+} vs. $f_{\text{H}_2\text{O}^+}$ and f_{O^+} vs. $f_{\text{H}_2\text{O}^+}$ for all the
7 laboratory standards. The empirical estimate used in the default AMS fragmentation
8 table (Allan et al., 2004) for the $\text{OH}^+/\text{H}_2\text{O}^+$ ratio is very consistent with the observed
9 relative intensities, indicating that the OH^+ ion indeed arises from the fragmentation of
10 molecular water from thermal decomposition of the standards. The consistency in these
11 fragmentation patterns also holds for various chamber SOA (Chen et al., 2011). The
12 $\text{O}^+/\text{H}_2\text{O}^+$ ratio, in contrast, shows substantial scatter, as the dominant source of the O^+ for
13 our standards appears to be fragmentation of CO_2^+ rather than H_2O^+ (Fig. S4c.).
14 Alcohols, which do not produce CO_2^+ , are an exception with $\text{O}^+/\text{H}_2\text{O}^+$ ratios that are
15 much closer to the empirical estimates. Fragmentation of CO_2^+ to yield O^+ ($\text{O}^+/\text{CO}_2^+ \sim$
16 6%) is currently not accounted for in the AMS elemental ratio analysis and will
17 contribute to the underestimation observed in AMS O:C values.

18 **3.3 Measurements of H_2O^+ , CO^+ and CO_2^+ with VUV Ionization**

19 The H_2O^+ , CO_2^+ , and CO^+ signals observed in the AMS are produced by dehydration and
20 decarboxylation processes that take place before ionization (i.e. on the vaporizer surface
21 or in the gas-phase after evaporation) and/or after 70 eV electron-impact ionization (i.e.
22 fragmentation of thermally excited ions). VUV-AMS measurements were used to
23 examine the production mechanisms of these ions in more detail. VUV-AMS data were
24 obtained for many standards with the AMS vaporizer set to both 200°C and 600°C (See
25 Table 1). All experiments were carried out under an argon atmosphere. A VUV-AMS
26 spectrum of glutaric acid is shown in Fig. 4a as an example. This spectrum was observed
27 with the AMS vaporizer at 200°C and a VUV photon energy of 10.5 eV. Since VUV is a
28 "softer" ionization method than EI, this spectrum would be expected to contain only the
29 glutaric acid molecular ion if thermal decomposition on the vaporizer was negligible.

1 However, even at this lower vaporizer temperature, the molecular ion of glutaric acid
2 (m/z 132) has very low intensity and organic ion fragments corresponding to loss of
3 neutral H₂O, CO, and CO₂ from glutaric acid are observed instead. CO₂⁺, CO⁺, and H₂O⁺
4 are negligible in this spectrum at this VUV photon energy.

5 Figure 4b shows the CO₂⁺, CO⁺, and H₂O⁺ signals observed from glutaric acid as a
6 function of VUV energy. The onsets of CO₂⁺, CO⁺, and H₂O⁺ signals are observed to
7 occur at VUV energies that correspond to the ionization energies of neutral H₂O, CO₂,
8 and CO molecules (12.62 eV, 13.77 eV, and 14.01 eV respectively), rather than the 10.5
9 eV ionization energies of the observed organic ions. This indicates that these ions are formed
10 by VUV ionization of neutral CO₂, CO, and H₂O molecules rather than by dissociative
11 ionization of glutaric acid. Neutral CO₂, CO, and H₂O fragments formed upon
12 photoionization of glutaric acid could further ionize to give rise to these signals. This process
13 requires the absorption of two photons in the ionization region, however, and is therefore
14 unlikely. Instead, the most likely source of CO₂⁺, CO⁺, and H₂O⁺ signals is direct VUV
15 ionization of neutral CO₂, CO, and H₂O molecules formed from thermal decomposition of
16 organic species on the AMS vaporizer. VUV-AMS measurements of the other organic
17 standards also show a lack of parent ions and fragments corresponding to loss of CO₂, CO,
18 or H₂O moieties (see Fig. S2), indicating that a wide range of oxidized organic species
19 undergo dehydration and decarboxylation upon heating to temperatures greater than
20 200°C.

21 **3.4 Effect of Vaporizer Temperature on H₂O⁺, CO⁺ and CO₂⁺**

22 Thermal denuder measurements have shown that ambient OA needs to be heated to a
23 minimum temperature of ~225°C for several seconds in order to insure quantitative
24 vaporization of a significant fraction of ambient oxidized OA (Huffman et al., 2009).
25 Figure S3 compares the trends in $f_{\text{H}_2\text{O}^+}$, f_{CO^+} and $f_{\text{CO}_2^+}$ observed with the AMS (using EI)
26 at vaporizer temperatures of 600°C and 200°C. The total CO₂⁺/CO⁺/H₂O⁺ decomposition
27 fragment intensities observed for both temperatures is remarkably similar across the
28 standards. In most cases, $f_{\text{H}_2\text{O}^+}$ is slightly higher at 200°C compared to 600°C, while f_{CO^+}
29 follows the opposite trend and $f_{\text{CO}_2^+}$ changes little between the two temperatures. This

1 indicates that dehydration is facile for these acids and alcohols even at 200°C, which is
2 also consistent with the VUV results shown in Fig. 4. The extent of thermal
3 decomposition observed in the AMS is likely influenced by its specific vaporization
4 conditions (i.e. porous tungsten hot surface and high-vacuum conditions). For example,
5 Lloyd and Johnston (2009) reported that in laser-desorption–electron-ionization analysis
6 of SOA, the signal due to CO_2^+ was much lower than in AMS spectra of the same aerosol
7 type, and attributed the difference to differences in the vaporization conditions. Our
8 measurements suggest that thermally-induced decomposition could affect the
9 interpretation of organic measurements from other aerosol chemistry measurement
10 techniques that utilize thermal desorption on surfaces, even if temperatures of only 200°C
11 are reached. Such techniques include aerosol Gas Chromatography-Mass Spectrometry
12 (GC-MS) and thermal-desorption Chemical Ionization mass Spectrometry (CIMS) (e.g.
13 (Lopez-Hilfiker et al., 2014; Williams et al., 2006; Yatavelli and Thornton,
14 2010; Holzinger et al., 2013). Proton Transfer Reaction – Mass Spectrometry (PTR-MS)
15 measurements of heated ambient filters by Holzinger et al. (2010), for example, show low
16 molecular weight fragments at higher thermal desorption temperatures, consistent with
17 this finding. The specific impact of the surface materials, vaporization temperatures, and
18 pressure conditions on the decomposition reactions of OA should be the focus of future
19 studies.

20 **3.5 Improved-Ambient method**

21 It is clear from Fig. 3 that the relationships among $f_{\text{CO}_2^+}$, $f_{\text{H}_2\text{O}^+}$, and f_{CO^+} are variable and
22 cannot be well prescribed with a single empirical relationship. Furthermore, as discussed
23 in sections 3.2 and 3.3, O:C and H:C calculated with the Aiken-Ambient method are
24 biased low because the empirical estimates used in this method often underestimate the
25 intensities of the H_2O^+ and/or CO^+ fragments. Acidic species are observed to be a large
26 source for CO^+ and H_2O^+ fragments while alcohols are a significant source of H_2O^+
27 fragments.

28 A correction that is dependent on both acid and alcohol content of the OA is needed to
29 address this composition dependence in the OA fragmentation. Previous AMS

1 measurements have shown that $f_{\text{CO}_2^+}$, can be used as a surrogate for acid content
 2 (Duplissy et al., 2011; Takegawa et al., 2007). An AMS surrogate for alcohol moieties
 3 has not been identified before, but spectra obtained during this study indicate that f_{CHO^+}
 4 (m/z 29) can be used as a surrogate for alcohol content. As shown in Fig. S5, spectra of
 5 standard species with no alcohol content have minimal $f_{\text{CHO}^+} < 0.05$ while those with non-
 6 zero alcohol content show f_{CHO^+} values ranging from 0.05 to 0.15. High f_{CHO^+} values are
 7 found for polyols as well as multifunctional species with non-acid OH groups. Some
 8 esters are also observed to yield f_{CHO} similar to species with non-acid OH groups. The
 9 cleavage of aldehydes to give CHO^+ is not generally observed to be important
 10 (McLafferty and Turecek, 1993). Previous studies have shown that CHO^+ is also an
 11 atmospherically significant ion and a key oxygen-containing ion in many types of
 12 ambient and chamber aerosol (Ng et al., 2010a). The f_{29} (f_{CHO^+}) fragment has also been
 13 used to monitor photooxidation of glyoxal and related species in the aqueous phase (Lee
 14 et al., 2011). Based on these results, a composition-dependent correction factor with a
 15 linear dependence on $f_{\text{CO}_2^+}$ and f_{CHO^+} was examined. While the CHO^+ fragment is easily
 16 resolved from the isobaric C_2H_5^+ organic fragment in high-resolution AMS spectra, it
 17 overlaps with $^{15}\text{N}^{14}\text{N}^+$ fragments from N_2 in air. Thus, a background correction must be
 18 used in order to obtain an accurate value of f_{CHO^+} . AMS data acquired while sampling
 19 through a particle filter can be used to obtain the information needed for such a
 20 background correction (as is already necessary for the accurate determination of $f_{\text{CO}_2^+}$).

21 We performed a multiple linear regression between the known elemental ratios of the OA
 22 standards and those determined from Eqs. (1) and (2) to obtain the best-fit constants and
 23 coefficients as follows:

$$24 \quad \text{O:C}_{\text{I-A}} = \text{O:C}_{\text{A-A}} \times [1.26 - 0.623 \times f_{\text{CO}_2^+} + 2.28 \times f_{\text{CHO}^+}] \quad (6)$$

$$25 \quad \text{H:C}_{\text{I-A}} = \text{H:C}_{\text{A-A}} \times [1.07 + 1.07 \times f_{\text{CHO}^+}] \quad (7)$$

26 In the equations above the Improved-Ambient (I-A) elemental ratios are expressed as a
 27 product of Aiken-Ambient (A-A) elemental ratios and a composition-dependent
 28 correction factor. This allows for simple recalculation of the Improved-Ambient
 29 elemental ratios from Aiken-Ambient values without the need for performing a re-

1 analysis of the raw mass spectra and can be easily applied to already published AMS
2 results.

3 Figures 1e and 1f show the O:C and H:C values obtained for the standards after using the
4 Improved-Ambient method in Eqs. (6) and (7). The corrections remove the systematic
5 O:C underestimation seen in Fig. 1c for the multi-functional species. The diacids and
6 alcohols are still biased low in O:C, but the bias has been reduced. The errors in the O:C
7 and H:C elemental ratios calculated for the standards with the Improved-Ambient method
8 are 28% and 13% respectively. Smaller errors (8%) are observed for the values of
9 OM:OC using the Improved-Ambient method (see Fig. S6).

10 Figure 5a compares the approximate carbon oxidation state values calculated from the
11 Improved-Ambient elemental ratios and the known standard elemental ratios of the
12 organic standards. The two sets of values agree with a standard deviation of $0.5 \overline{OS}_C$
13 units. The largest deviations are observed for the laboratory standards whose Improved-
14 Ambient O:C values are biased lower than the known values. Figure 5b shows a
15 comparison between the \overline{OS}_C values calculated for the standard molecule data using the
16 Aiken-Ambient and Improved-Ambient methods. The error bars on the standard data
17 indicate the estimated uncertainty in the calculated Aiken-Ambient \overline{OS}_C values (using
18 propagation of O:C (H:C) errors of 28% (14%) observed for multifunctional species
19 with Aiken-Ambient method). In general, the agreement between the Aiken-Ambient
20 \overline{OS}_C values and the Improved-Ambient \overline{OS}_C values is much better than the propagated
21 errors. This indicates that the oxidation state values derived from AMS data (and
22 potentially from other techniques using thermal desorption MS) are more robust and less
23 variable than measured values of H:C and O:C.

24 The robustness of the \overline{OS}_C parameter is largely due to its invariance with respect to
25 dehydration (and hydration) processes (Kroll et al., 2011). The \overline{OS}_C value that is
26 currently calculated from AMS spectra is not strictly invariant with respect to hydration
27 and dehydration because the AMS fragmentation table neglects small amounts of H^+
28 formed from fragmentation of H_2O^+ ions (Hildebrandt Ruiz, 2014). Other fragments,
29 such as OH^+ , and O^+ are properly accounted for as discussed above. Figure 5a shows the

1 effect of calculating Improved-Ambient $\overline{\text{OS}}_{\text{C}}$ values with a fragmentation table that
2 includes the H^+ fragment (see Supplementary Information for details). The Hildebrandt
3 Ruiz (2014) correction results in slightly smaller $\overline{\text{OS}}_{\text{C}}$ values than obtained with the
4 default AMS fragmentation table due to a small (<3%) increase in the Improved-Ambient
5 H:C.

6 **3.6 Estimated accuracy of the Improved-Ambient method for Mixtures**

7 The errors observed in the Improved-Ambient elemental ratios of individual OA
8 standards are expected to be upper limits for the corresponding errors in mixtures, where
9 inaccuracies in individual molecule predictions can compensate for each other. The
10 expected improvement in accuracy for mixtures is investigated here for randomly
11 generated theoretical mixtures of the OA standard molecules.

12 Theoretical standard mixtures were generated by combining equimolar fractions of up to
13 25 different individual OA standards. Each mixture of individual standards is expressed
14 as $\sum_i n_i \text{C}_{x_i} \text{H}_{y_i} \text{O}_{z_i}$ where n_i is the mole fraction of standard i in the mixture, and x_i , y_i , and
15 z_i are the number of C, H, and O atoms within a molecule of standard i . The O:C ratio
16 for any given mixture is calculated as follows:

$$17 \quad \text{O:C}_{\text{mix(I-A)}} = \sum_i (\text{O:C}_i (\text{I-A}) \times n_i x_i) / \sum_i (n_i x_i) \quad (8)$$

$$18 \quad \text{O:C}_{\text{mix(Molecular)}} = \sum_i (\text{O:C}_i (\text{molecular}) \times n_i x_i) / \sum_i (n_i x_i) \quad (9)$$

19 H:C ratios are calculated analogously with the appropriate substitutions in Eqs. (8) and
20 (9). For each type of mixture, 1000 different randomly generated versions were
21 examined and the average absolute value of relative errors in the calculated Improved-
22 Ambient elemental ratios over all 1000 variants is calculated for each mixture. For the
23 1000 mixtures made of 25 standards, the O:C ratios ranged from 0.3 to 0.83 and the H:C
24 ratios ranged from 1.36 to 1.92. The mixtures made of 10 standards covered a wider
25 range of O:C ratios (0.18 to 1.02) and H:C ratios (1.15-2.02). For comparison, the
26 average Improved-Ambient O:C(H:C) values of LV-OOA are 0.84 (1.43) and of SV-
27 OOA are 0.53(1.62). Thus, the elemental ratios of the organic standard mixtures cover
28 the range of ambient observations.

1 Figures 6 a and b show the error in Improved-Ambient O:C and H:C values as a function
2 of the number of standard molecules in the mixture of interest. It is clear from the figure
3 that the error becomes smaller and plateaus for both of the elemental ratios as the number
4 of OA species in the mixture is increased. For O:C and H:C the errors decrease from
5 28% to 12% and 13% to 4% respectively as the number of species in the mixture is
6 increased. The plateau in the error is already reached for both elemental ratios by the time
7 that only 10 different standard OA species are added together. Ambient OA is a complex
8 mixture of hundreds of individual species. If the standard molecule mixtures are
9 reasonably representative of ambient OA mixtures, these results indicate that the
10 Improved-Ambient O:C and H:C values calculated for ambient OA and SOA have errors
11 close to ~12% and ~4%, respectively.

12 **3.7 Effect of Improved-Ambient method on previous measurements of** 13 **AMS Elemental Ratios**

14 Given the large number of AMS datasets that have reported OA elemental ratios
15 calculated with the Aiken-Ambient technique, it is useful to examine the impact that the
16 proposed corrections will have on existing results and their interpretation.
17 We focus on several HR-AMS datasets that have been analyzed with the Aiken-Ambient
18 method and for which elemental ratios have been reported in the literature, and/or for
19 which HR spectra are available on the HR-AMS spectral database
20 (<http://cires.colorado.edu/jimenez-group/HRAMSsd/>).

21 For ambient datasets, elemental ratios have been previously reported for total OA as well
22 as OA components (i.e. groups of organic species that represent different OA sources and
23 or processes). Primary OA (POA) species are directly emitted into the atmosphere while
24 secondary OA (SOA) are species formed as a result of atmospheric transformation
25 (Ulbrich et al., 2009; Zhang et al., 2011; Lanz et al., 2007). Several types of POA have
26 been identified, including hydrocarbon-like organic aerosol (HOA), which is associated
27 with fossil fuel combustion and other urban sources, biomass burning OA (BBOA),
28 cooking OA (COA), and other OA from local sources (LOA) (Zhang, et al., (2011) and
29 references therein). SOA species, which generally dominate ambient OA mass
30 concentrations, consist of a continuum of oxidized organic aerosol species (OOA); that

1 reflect differences in extent and mechanisms of photochemical aging as well as precursor
2 sources (Ng et al., 2010b; Jimenez et al., 2009). Two broad types of ambient SOA,
3 denoted as LV-OOA (low volatility oxidized organic aerosol) and SV-OOA (semi-
4 volatile oxidized organic aerosol), have been identified at many locations. LV-OOA
5 represent the more highly oxidized organic aerosol while SV-OOA are the less oxidized
6 OA.

7 Figure 7 shows the average O:C, H:C, OM:OC and \overline{OS}_C values obtained when
8 previously published field and chamber SOA data are analyzed using the Improved-
9 Ambient method. Aiken-Ambient values are shown for all data and Aiken-Explicit
10 values are shown for the chamber SOA. The data for Fig. 7 are available in Table 3 and
11 the detailed values for each field dataset are in Supplementary Tables 1 and 2. The
12 Improved-Ambient elemental ratios of chamber SOA are higher than previously reported
13 Aiken-Ambient values and the relative change varies with the identity of the precursor.
14 For the α -pinene + O₃ and β -caryophyllene + O₃ SOA (Chen et al., 2011)), the predicted
15 increase in O:C (H:C) is smaller than that for the isoprene + OH (Chen et al., 2011) and
16 toluene + OH SOA (Hildebrandt Ruiz, 2014). These differences are likely linked to the
17 specific molecular functionalities associated with SOA formed from each precursor.
18 Isoprene SOA, for example, is known to produce organic peroxides (Surratt et al., 2006)
19 acids (Fisseha et al., 2004). The largest increases are comparable to those observed for
20 the standard molecules with diacid and polyol functionalities while the smaller increases
21 are consistent with those observed for multifunctional standards. The Improved-Ambient
22 elemental ratios of ambient OA (individual components as well as total OA) generally lie
23 at the high error limit of the Aiken-Ambient values. The Improved-Ambient O:C and
24 H:C values of total OA, for example are larger than the corresponding Aiken-Ambient
25 values by approximately 27% and 11% on average. These relative differences are similar
26 to those observed for the multifunctional OA standards (Fig. 1c) and smaller than those
27 observed for some of the individual chamber SOA systems or individual SOA standards.

28 Figure 7 shows that chamber SOA elemental ratios calculated with the Improved-
29 Ambient method agree well with those calculated using the Aiken-Explicit method. This
30 agreement is important since it confirms that the Improved-Ambient method compares

1 well with the Aiken-Explicit method not only for laboratory standards but also for OA
2 mixtures with complex compositions and molecular functionalities that cannot be readily
3 duplicated with commercial standards. Recently, agreement between gas and particle
4 phase elemental ratio measurements of highly oxidized, extremely low-volatility organic
5 species (ELVOC) formed in the α -pinene + O₃ reaction has also been demonstrated (Ehn
6 et al., 2014). This agreement was found when low-volatility oxidized products (ELVOC)
7 were measured as individual molecules in the gas phase using CIMS and as condensed
8 particle phase species using AMS and the Improved-Ambient method. The proposed
9 auto-oxidation mechanism in Ehn et al (2014) indicates that the ELVOC probably have
10 multiple hydroperoxide moieties. Though hydroperoxides are not represented in the
11 calibration set, the agreement between the individually identified ELVOC compounds
12 measured in Ehn et al and the O:C of low-concentration α -pinene SOA obtained from
13 AMS data using the Improved method describe here is encouraging.

14 While the Improved-Ambient only corrects the elemental ratio values obtained with the
15 AMS, the resulting increase in both O:C and H:C values implies an increase in organic
16 mass as well. On average, the OM:OC ratios obtained with the Improved-Ambient
17 method for total OA are 9% higher than previously published Aiken-Ambient values.
18 The average Improved-Ambient OM:OC ratio of total OA is 1.84 with variation from
19 1.3-1.5 for primary OA components to 1.8-2.2 for secondary OA components; chamber
20 SOA Improved-Ambient OM:OC ratios vary with precursor. The OM:OC ratio of the
21 ambient OOA components is consistent with water soluble fraction of aged ambient
22 aerosol, which has been measured by other techniques to be in the range of 2.1 (Turpin
23 and Lim, 2001) to 2.54 (Polidori et al., 2008). A fit of the Improved-Ambient OM:OC
24 data results in the following empirical relationship (see Fig. S5):

$$25 \quad \text{OM:OC}_{\text{I-A}} = 1.29 \times \text{O:C}_{\text{I-A}} + 1.17 \quad (10)$$

26 In Fig. 7 it is important to note that the carbon oxidation state of total OA calculated with
27 the Improved-Ambient method remains relatively unchanged from that determined by the
28 Aiken-Ambient method (Improved_Ambient $\overline{\text{OS}}_{\text{C}}$ is higher by only 0.06). The $\overline{\text{OS}}_{\text{C}}$
29 values from the two methods also agree closely even for the chamber systems that display
30 larger differences in O:C and H:C values (see Fig. 7). This reinforces the conclusion that

1 \overline{OS}_C is a more robust measure of OA oxidation levels than either O:C or H:C since is not
2 affected by hydration or dehydration processes taking place in the atmosphere or during
3 the measurement process and is thus also not sensitive to other sources of H₂O in aerosol
4 samples such as aerosol water or dehydration of inorganic acids (Kroll et al., 2011).

5 The corrected elemental analysis values will have implications for the interpretation of
6 Van Krevelen diagrams (i.e. plots of H:C vs O:C), which have been used to obtain
7 insights into the chemical transformations of ambient OA. Heald et al., (2010) first
8 showed the utility of this diagram for bulk total OA (including POA and SOA)
9 composition analysis, and demonstrated that for some datasets bulk ambient OA evolved
10 with a slope of -1, suggesting composition changes with aging that are consistent with
11 simultaneous increases in both carbonyl and alcohol moieties. Ng et al. (2011) used the
12 Van Krevelen diagram to follow the oxidative transformations of ambient OOA (as
13 opposed to total OA) from multiple field campaigns and showed that they clustered along
14 a slope of approximately -0.5. This slope was interpreted as being indicative of simple
15 oxidative mechanisms that involve net additions of both C(O)OH *and* -OH/-OOH
16 functional groups without fragmentation (i.e. C-C bond cleavage), and/or the addition of
17 C(O)OH groups with fragmentation. Van Krevelen plots of ambient and chamber SOA
18 species from Table 3 are shown in Fig. S7. The Improved-Ambient method yields Van
19 Krevelen slopes that are approximately 20% shallower than those determined with the
20 Ambient-Aiken method. Details are discussed in Chen et al. 2014 (manuscript in
21 preparation). These slopes (-0.8 for total OA, and -0.4 for OOA) suggest that the ambient
22 OA oxidative mechanisms involve different net addition of -OH and/or -OOH
23 functionalities and fragmentation than previously assumed.

24 **3.8 Effect of Improved-Ambient method on empirical parameterizations of** 25 **OA elemental ratios from unit mass resolution data**

26 Empirical methods relating unit mass resolution (UMR) AMS ion tracers with Ambient-
27 Aiken elemental ratios obtained from high-resolution AMS data have been previously
28 reported by Aiken et al. (2008) and Ng et al. (2011). Here we reassess these relationships
29 for elemental ratios calculated with the Improved-Ambient method.

1 Aiken et al. (2008) presented a parameterization to estimate O:C from measured f_{44}
2 values. High-resolution AMS measurements indicate that the UMR signal at m/z 44 is
3 mostly due to CO_2^+ , although $\text{C}_2\text{H}_4\text{O}^+$ can play a role in some cases (e.g. isoprene SOA
4 and BBOA). Figure 8a shows Improved-Ambient O:C values for standard, chamber, and
5 ambient field data vs. f_{44} . A linear fit of the field OA components (primary and
6 secondary) provides the following parameterization for Improved-Ambient O:C values:

$$7 \quad \text{O:C}_{\text{I-A}} = 0.079 + 4.31 \times f_{44} \quad (11)$$

8 Equation (11) reproduces most of the data points including all the ambient OA
9 components obtained by factor analysis. The O:Cs calculated with Eq. (11) reproduce
10 measured secondary OA component values with an error of 13%. The agreement for
11 primary OA components is not as good, indicating that the accuracy of Eq. (11) is
12 reduced when f_{44} is small (<4% on average). The outliers in Fig. 6a correspond to species
13 with low acid content and high alcohol content (i.e., polyols, and other multifunctional
14 species with OH groups). Thus, the inferred O:C values for some types of marine
15 aerosols that have been shown to contain alcohol functionalities (Hawkins and Russell,
16 2010) may be somewhat underpredicted. The chamber data outliers in Fig. 8a also
17 indicate that Eq. (11) may underpredict O:C values substantially in ambient environments
18 dominated by NO_x -free isoprene chemistry and toluene chemistry.

19 Ng et al. (2011) derived a method for estimating H:C values of OOA components and
20 SOA species from f_{43} . This parameterization was based on ambient OOA components
21 and chamber SOA species with $f_{44} > 0.05$ and $f_{43} > 0.04$. For these species, m/z 43 is
22 typically dominated by $\text{C}_2\text{H}_3\text{O}^+$. Only a few of the measured multifunctional standards
23 yield mass spectra which fall within these prescribed valid ranges. Since these few data
24 points do not add enough significant information to derive a new parameterization, we
25 use them together with chamber and field data to evaluate a scaled version of the Ng et al.
26 (2011) relationship. We choose a scaling factor of 1.11 since the Improved-Ambient
27 method increases the H:Cs of ambient OA by 11% on average. The resulting scaled
28 parameterization is as follows:

$$29 \quad \text{SOA H:C}_{\text{I-A}} = 1.12 + 6.74 \times f_{43} + 17.77 \times f_{43}^2 \quad (12)$$

30 Figure 8b compares the parameterization from Eq. (12) with the measured Improved-
31 Ambient H:C values. The figure indicates that as in Ng et al. (2011), the measured H:C

1 values for secondary OA components, secondary chamber OA, and several standard
2 molecules are reproduced to within $\pm 10\%$ by Eq. (12).

3 **3.9 Atmospheric Implications**

4 Aerosol elemental ratios measured with the AMS have been previously used to
5 distinguish between different types of organic aerosol (Jimenez et al., 2009;Ng et al.,
6 2010), examine the degree to which chamber SOA is able to simulate ambient SOA
7 (Chhabra et al., 2010;Ng et al., 2010), and to constrain oxidation mechanisms used in
8 theoretical models (Jimenez et al., 2009;Kroll et al., 2011; Donahue et al., 2011; Daumit
9 et al., 2013; Chen et al., 2014). Here we show that while the changes introduced by the
10 Improved-Ambient method can be significant, they do not change any fundamental
11 conclusions made from previous AMS studies.

12 As shown in Fig. 7, I-A elemental ratios for ambient OA components have the same
13 trends with respect to each other as previously published A-A elemental ratios. The
14 relative levels of oxidation for the various OA components, for example, do not change
15 with respect to each other. The OOA components still span a continuum of oxidation
16 levels; LV-OOA components remain more oxidized than SV-OOA components and OOA
17 components and more oxidized than the various POA components (Jimenez et al., 2009).
18 In fact, the Improved-Ambient method enhances previous conclusions about the high
19 degree of oxygenation of atmospheric OOA, indicating that ambient OA has a greater
20 oxygen content than suggested by previous AMS studies.

21 Laboratory chamber studies provide the ideal means of simulating ambient aerosol
22 formation and aging processes under controlled and reproducible experimental conditions
23 (i.e. selected reactants, photochemical conditions, and aging times). However, previous
24 work has shown that laboratory chamber studies are unable to generate SOA or
25 photochemically aged OA with the same chemical composition as the LV-OOA species
26 observed in the atmosphere (Chhabra et al., 2010;Ng et al., 2010). The elemental ratios
27 obtained with I-A method reconfirm this difference. Figure 7 shows, for example, that
28 the I-A elemental ratios observed for the SOA from terpene and sesquiterpene precursors
29 are significantly less oxidized than the average ambient LV-OOA component. In fact,

1 the terpene and sesquiterpene chamber SOA generally only reach the O:C and OSc
2 values observed for the less oxidized SV-OOA components. As shown in Table 2, the I-
3 A elemental ratios of isoprene and toluene SOA experience large changes compared to
4 their corresponding A-A values. These changes are large enough to bring the O:C and
5 OSc values of these SOA in good agreement with LV-OOA values. However, as shown
6 in Fig. 4a, the oxygen containing functional groups in these SOA still do not reproduce
7 the mass spectral signatures obtained from ambient LV-OOA. Thus, the gap in the AMS
8 chemical compositions measured for chamber and ambient SOA remains even when the
9 I-A method is used.

10

11 Many studies have used elemental ratios (O:C and H:C) or the oxidation state values
12 derived from them as key constraints to understand how OA chemical composition
13 evolves in the atmosphere. Some two dimensional chemical spaces that directly use these
14 parameters as constraints are: the van Krevelen space discussed in section 3.7 of this
15 manuscript, OSc vs. carbon number, and OSc vs. saturation vapor concentration (Jimenez
16 et al., 2009; Kroll et al., 2011; Donahue et al., 2011). Daumit et al. (2013) have used a
17 three dimensional space (carbon number, O:C, H:C) to constrain and define the
18 chemically feasible back-reactions that could lead to the oxidized LV-OOA species
19 observed in the atmosphere. In all of these spaces the measured bulk values of O:C, H:C,
20 and OSc provide mechanistic insight by limiting the reaction pathways and intermediates
21 that are potentially possible. Daumit et al. (2013) have compared the difference in
22 constraints introduced when LV-OOA elemental ratios are calculated using A-A and I-A
23 methods (The I-A elemental ratios in Daumit et al. (2013) were calculated by scaling A-
24 A_O:C and H:C ratios by 1.3 and 1.11, respectively). For the same LV-OOA volatility,
25 elemental ratios obtained with the I-A method constrain the LV-OOA composition to
26 contain a higher hydroxyl/carbonyl ratio than the elemental ratios obtained with the A-A
27 method. Since hydroxyl groups result in lower volatility than carbonyl groups, this
28 implies that the average LV-OOA carbon number calculated using the I-A constraints is
29 lower than that calculated using A-A constraints. From the standpoint of chemical
30 mechanisms, this also means that the new I-A constraints will result in the need for new
31 reactions that produce more hydroxyl groups relative to carbonyl groups. This is

1 consistent with the general trend noticed in the van Krevelen diagrams (see section 3.7)
2 which indicate that ambient OA oxidation increases O:C while maintaining high H:C
3 values. This suggests that models should explore different and or additional mechanisms
4 for adding -OH and/or -OOH functionalities during oxidation of ambient OA.

5 **4 Conclusions**

6 This manuscript evaluates the accuracy of the AMS elemental analysis approach over a
7 wider range of OA species than has been studied before. Thermally-induced dehydration
8 and/or decarboxylation of OA species is observed to be efficient in the AMS not only at
9 the standard vaporizer temperature of 600°C but also at much lower vaporizer
10 temperature (even 200°C, the lowest feasible vaporization temperature). These processes
11 likely also play a role in other heated surface vaporization-based aerosol measurement
12 techniques even if they limit heating to ~200°C. The H₂O, CO, and CO₂ molecules
13 produced by these decomposition processes must be taken into account in order to obtain
14 accurate elemental composition information.

15 The accuracy of elemental ratios obtained with the AMS depends on the exact method
16 that is used. The Aiken-Explicit method reproduces known O:C and H:C ratios to within
17 20% and 12% respectively. These results validate the use of this methodology for
18 calculating elemental ratios across a range of OA molecular compositions. This method
19 is recommended for laboratory experiments and smog-chamber measurements as well as
20 ambient measurements when sufficient signal is available (e.g. at very polluted sites).
21 Careful control of the sampling conditions and/or calibration experiments that enable
22 unambiguous extraction of the organic signal contributions to measured H₂O⁺ and CO⁺
23 ion intensities are recommended for these situations (See for example Chen et al. (2011)).
24 The Aiken-Ambient method (used for most measurements of aerosols obtained in air)
25 produces O:C (H:C) ratios for multifunctional species that are within 28% (14%) of
26 known ratios respectively. These values are biased low, however, with larger biases
27 observed for some highly functionalized species (e.g., polyols and polycarboxylic acids).
28 Detailed analysis of the AMS spectra indicate that these biases are largely due to the use
29 of empirically estimated intensities for H₂O⁺ and CO⁺ ions that are lower than the
30 actual measured values for these ions. An Improved-Ambient method for calculating

1 elemental ratios from OA is developed as part of this study and is recommended for
2 measurements obtained in air. This method combines the Aiken-Ambient results together
3 with correction factors that uses specific ion fragments as markers to reduce
4 composition-dependent bias and produce O:C (H:C) values for the standard molecules
5 that are within 28% (13%) of the known molecular values. Future work should include
6 comparisons between the OA elemental ratios obtained with the Improved-Ambient
7 technique and other elemental analysis techniques.

8 Application of the Improved-Ambient elemental analysis to previously published ambient
9 datasets results in an average increase of the O:C and H:C values of total OA by 27% and
10 11% respectively; The OM:OC ratios of total organic correspondingly increases by 9%.
11 The oxidation state values calculated with the Aiken-Ambient and Improved-Ambient
12 methods, on the other hand, do not differ substantially, since \overline{OS}_C is invariant with
13 respect to hydration and dehydration processes. This indicates that \overline{OS}_C is a more robust
14 parameter for monitoring oxidation of aerosols than either O:C or H:C; comparisons
15 between \overline{OS}_C measurements from the AMS and other elemental analysis techniques are
16 needed to investigate this in more detail.

17 The Improved-Ambient method indicates that the oxygen content of ambient OA is larger
18 than reported by previous AMS measurements. The chemistry involved in the formation
19 of highly oxidized ambient OOA is still poorly characterized, and chemical pathways that
20 produce high values of O:C are unclear. Thus, more work is required to develop and
21 explore alternative chemical mechanisms and modeling methods for simulating the
22 formation of highly oxidized ambient OA. The Van-Krevelen slope resulting from the
23 Improved-Ambient formulation is also shallower than previously reported (-0.8 for total
24 OA, and -0.4 for OOA). Aging mechanisms of ambient OA that qualitatively involve
25 greater net addition of -COH and -COOH groups relative to -CO groups should be
26 explored.

27 **Acknowledgements**

28 We thank the participants of AMS Clinic and AMS Users Meetings, Paul Ziemann, and
29 Colette Heald for many useful discussions on these topics. JHK, MRC, and DRW
30 acknowledge support from NSF CHE-1012809. JLJ was partially supported by NSF

1 AGS-1243354, NASA NNX12AC03G and NOAA NA13OAR4310063. QC is supported
2 by the National Science Foundation (ATM- 1238109) NMD is supported by the National
3 Science foundation (AGS1136479). KRW and the Chemical Dynamics Beamline
4 (Advanced Light Source) are supported by the Office of Basic Energy Sciences of the
5 U.S. Department of Energy under Contract No. DE-AC02-05CH11231. KRW. is
6 additionally supported by the Department of Energy, Office of Science Early Career
7 Research Program. E. F., L. R.W., and J. T. J. acknowledge support from the US Department
8 of Energy (DE-FG02-03ER83599, DE-FG02-05ER84269, DE-FG02-07ER84890)"

9

10

1 **References**

- 2 Aiken, A. C., DeCarlo, P. F., and Jimenez, J. L.: Elemental Analysis of Organic Species
3 with Electron Ionization High-Resolution Mass Spectrometry, *Anal. Chem.*, 79, 8350-
4 8358, doi:8310.1021/ac071150w, 2007.
- 5 Aiken, A. C., DeCarlo, P. F., Kroll, J. H., Worsnop, D. R., Huffman, J. A., Docherty, K.,
6 Ulbrich, I. M., Mohr, C., Kimmel, J. R., Sueper, D., Sun, Y., Zhang, Q., Trimborn, A.,
7 Northway, M., Ziemann, P. J., Canagaratna, M. R., Onasch, T. B., Alfarra, M. R., Prevot,
8 A. S. H., Dommen, J., Duplissy, J., Metzger, A., Baltensperger, U., and Jiménez, J. L.:
9 O/C and OM/OC Ratios of Primary, Secondary, and Ambient Organic Aerosols with a
10 High Resolution Time-of-Flight Aerosol Mass Spectrometer, *Environ. Sci. Technol.*, 42,
11 4478-4485, 2008.
- 12 Allan, J. D., Coe, H., Bower, K. N., Alfarra, M. R., Delia, A. E., Jiménez, J. L.,
13 Middlebrook, A. M., Drewnick, F., Onasch, T. B., Canagaratna, M. R., Jayne, J. T., and
14 Worsnop, D. R.: Technical note: Extraction of chemically resolved mass spectra from
15 Aerodyne aerosol mass spectrometer data, *J. Aerosol Sci.*, 35, 909-922, 2004.
- 16 Altieri, K. E., Turpin, B. J., and Seitzinger, S. P.: Composition of Dissolved Organic
17 Nitrogen in Continental Precipitation Investigated by Ultra-High Resolution FT-ICR
18 Mass Spectrometry, *Environ. Sci. Technol.*, 43, 6950-6955, 2009.
- 19 Bateman, A. P., Nizkorodov, S. A., Laskin, J., and Laskin, A.: Time-resolved molecular
20 characterization of limonene/ozone aerosol using high-resolution electrospray ionization
21 mass spectrometry, *Phys. Chem. Chem. Phys.*, 11, 7931-7942, 2009.
- 22 Canagaratna, M. R., Jayne, J. T., Jiménez, J. L., Allan, J. D., Alfarra, M. R., Zhang, Q.,
23 Onasch, T. B., Drewnick, F., Coe, H., Middlebrook, A., Delia, A., Williams, L. R.,
24 Trimborn, A. M., Northway, M. J., DeCarlo, P. F., Kolb, C. E., Davidovits, P., and
25 Worsnop, D. R.: Chemical and Microphysical Characterization of Ambient Aerosols with
26 the Aerodyne Aerosol Mass Spectrometer, *Mass Spectrom. Rev.*, 26, 185-222, 2007.

1 Chen, Q., Liu, Y. D., Donahue, N.M., Shilling, J. E., and Martin, S. T.: Particle-Phase
2 Chemistry of Secondary Organic Material: Modeled Compared to Measured O:C and
3 H:C Elemental Ratios Provide Constraints., *Environ. Sci. Technol.*, 45, 4763-4770, 2011.

4 Chen, Q., Heald, C. L., Jimenez, J. L., Canagaratna, M. R., Zhang, Q., He, L., Huang, X.,
5 Campuzano-Jost, P., Palm, B. B., Poulain, L., Martin, S. T., Abbatt, J. P. D., Lee, A. K.
6 Y., and Liggio, J.: Elemental Composition of Organic Aerosol: The Gap Between
7 Ambient and Laboratory Measurements, Submitted to *Geophys. Res. Lett.*, 2014.
8

9 Chhabra, P. S., Flagan, R. C., and Seinfeld, J. H.: Elemental analysis of chamber organic
10 aerosol using an aerodyne high-resolution aerosol mass spectrometer, *Atmos. Chem.*
11 *Phys.*, 10, 4111-4131, 2010.

12 Claeys, M., Graham, B., Vas, G., Wang, W., Vermeylen, R., Pashynska, V., Cafmeyer, J.,
13 Guyon, P., Andreae, M. O., Artaxo, P., and Maenhaut, W.: Formation of secondary
14 organic aerosols through photooxidation of isoprene, *Science*, 1173-1176, 2004.
15

16 Daumit, K. E., Kessler, S. H., and Kroll, J. H.: Average chemical properties and potential
17 formation pathways of highly oxidized organic aerosol, *Faraday Discussions*, 165, 181-
18 202,
19

20 DeCarlo, P. F., Kimmel, J. R., Trimborn, A., Northway, M. J., Jayne, J. T., Aiken, A. C.,
21 Gonin, M., Fuhrer, K., Horvath, T., Docherty, K., Worsnop, D. R., and Jiménez, J. L.: A
22 Field-Deployable High-Resolution Time-of-Flight Aerosol Mass Spectrometer, *Anal.*
23 *Chem.*, 78, 8281-8289, 2006.

24 Donahue, N. M., Epstein, S. A., Pandis, S. N., and Robinson, A. L.: A two-dimensional
25 volatility basis set: 1. organic-aerosol mixing thermodynamics, *Atmos. Chem. Phys.*
26 *Discuss.*, 11, 3303–3318, doi:3310.5194/acp-3311-3303-2011, 2011.
27

28 Duplissy, J., DeCarlo, P. F., Dommen, J., Alfarra, M. R., Metzger, A., Barmapadimos, I.,
29 Prevot, A. S. H., Weingartner, E., Tritscher, T., and Gysel, M.: Relating hygroscopicity

1 and composition of organic aerosol particulate matter, *Atmos. Chem. Phys.*, 11, 1155-
2 1165, 2011.

3 Ehn, M., Thornton, J. A., Kleist, E., Sipila, M., Junninen, H., Pullinen, I., Springer, M.,
4 Rubach, F., Tillmann, R., Lee, B., Lopez-Hilfiker, F., Andres, S., Acir, I.-H., Rissanen,
5 M., Jokinen, T., Schobesberger, S., Kangasluoma, J., Kontkanen, J., Nieminen, T.,
6 Kurten, T., Nielsen, L. B., Jorgensen, S., Kjaergaard, H. G., Canagaratna, M., Maso, M.
7 D., Berndt, T., Petaja, T., Wahner, A., Kerminen, V.-M., Kulmala, M., Worsnop, D. R.,
8 Wildt, J., and Mentel, T. F.: A large source of low-volatility secondary organic aerosol,
9 *Nature*, 506, 476-479, 2014.

10 Fisseha, R., Dommen, J., Sax, M., Paulsen, D., Kalberer, M., Maurer, R., H \ddot{a} ffler, F.,
11 Weingartner, E., and Baltensperger, U.: Identification of Organic Acids in Secondary
12 Organic Aerosol and the Corresponding Gas Phase from Chamber Experiments, *Anal.*
13 *Chem.*, 76, 6535-6540, 2004.

14

15 Gilardoni, S., Liu, S., Takahama, S., Russell, L. M., Allan, J. D., Steinbrecher, R.,
16 Jimenez, J. L., De Carlo, P. F., Dunlea, E. J., and Baumgardner, D.: Characterization of
17 organic ambient aerosol during MIRAGE 2006 on three platforms, *Atmos. Chem. Phys.*,
18 9, 5417-5432, 2009.

19 Hastings, W. P., Koehler, C. A., Bailey, E. L., and De Haan, D. O.: Secondary organic
20 aerosol formation by glyoxal hydration and oligomer formation: Humidity effects and
21 equilibrium shifts during analysis, *Environ. Sci. Technol.*, 39, 8728-8735, 2005.

22 Hawkins, L. N., and Russell, L. M.: Polysaccharides, proteins, and phytoplankton
23 fragments: four chemically distinct types of marine primary organic aerosol classified by
24 single particle spectromicroscopy, *Advances in Meteorology*, 2010, 612132, doi:
25 10.1155/2010/612132, 2010.

26

27 Heald, C. L., Kroll, J. H., Jimenez, J. L., Docherty, K. S., DeCarlo, P. F., Aiken, A. C.,
28 Chen, Q., Martin, S. T., Farmer, D. K., and Artaxo, P.: A simplified description of the

1 evolution of organic aerosol composition in the atmosphere, *Geophys. Res. Lett.*, 37,
2 L08803, doi:08810.01029/02010GL042737, 2010.

3 Hildebrandt Ruiz, L., Paciga, A. L., Cerully, K., Nenes, A., Donahue, N. M., and Pandis,
4 S. N.: Aging of Secondary Organic Aerosol from Small Aromatic VOCs: Changes in
5 Chemical Composition, Mass Yield, Volatility and Hygroscopicity, Submitted to
6 *Atmospheric Chemistry and Physics Discussions*, 2014.

7
8 Holzinger, R., Goldstein, A. H., Hayes, P. L., Jimenez, J. L., and Timkovsky, J.:
9 Chemical evolution of organic aerosol in Los Angeles during the CalNex 2010 study,
10 *Atmos. Chem. Phys.*, 13, 10125-10141, 2013.

11 Huffman, J. A., Docherty, K. S., Aiken, A. C., Cubison, M. J., Ulbrich, I. M., DeCarlo, P.
12 F., Sueper, D., Jayne, J. T., Worsnop, D. R., Ziemann, P. J., and Jimenez, J. L.:
13 Chemically-Resolved Aerosol Volatility Measurements from Two Megacity Field
14 Studies, *Atmos. Chem. Phys.*, 9, 7161-7182, 2009.

15 IPCC: *Climate Change 2013: The Physical Scientific Basis*, Cambridge University Press,
16 Cambridge, England, 2013.

17 Jimenez, J. L., Canagaratna, M. R., Donahue, N. M., Prevot, A. S. H., Zhang, Q., Kroll, J.
18 H., DeCarlo, P. F., Allan, J. D., Coe, H., Ng, N. L., Aiken, A. C., Docherty, K. S.,
19 Ulbrich, I. M., Grieshop, A. P., Robinson, A. L., Duplissy, J., Smith, J. D., Wilson, K. R.,
20 Lanz, V. A., Hueglin, C., Sun, Y. L., Tian, J., Laaksonen, A., Raatikainen, T., Rautiainen,
21 J., Vaattovaara, P., Ehn, M., Kulmala, M., Tomlinson, J. M., Collins, D. R., Cubison, M.
22 J., Dunlea, E. J., Huffman, J. A., Onasch, T. B., Alfarra, M. R., Williams, P. I., Bower,
23 K., Kondo, Y., Schneider, J., Drewnick, F., Borrmann, S., Weimer, S., Demerjian, K.,
24 Salcedo, D., Cottrell, L., Griffin, R., Takami, A., Miyoshi, T., Hatakeyama, S., Shimojo,
25 A., Sun, J. Y., Zhang, Y. M., Dzepina, K., Kimmel, J. R., Sueper, D., Jayne, J. T.,
26 Herndon, S. C., Trimborn, A. M., Williams, L. R., Wood, E. C., Middlebrook, A. M.,
27 Kolb, C. E., Baltensperger, U., and Worsnop, D. R.: Evolution of Organic Aerosols in the
28 Atmosphere, *Science*, 326, 1525-1529, 10.1126/science.1180353, 2009.

1 Kiss, G., Varga, B., Galambos, I., and Ganszky, I.: Characterization of water-soluble
2 organic matter isolated from atmospheric fine aerosol, *Journal of Geophysical Research:*
3 *Atmospheres* 107, ICC 1-1-ICC 1-8, 2002.

4 Krivacsy, Z., Gelencser, A., Kiss, G., Meszaros, E., Molnar, A., Hoffer, A., Meszaros, T.,
5 Sarvari, Z., Temesi, D., and Varga, B.: Study on the chemical character of water soluble
6 organic compounds in fine atmospheric aerosol at the Jungfraujoch, *Journal of*
7 *Atmospheric Chemistry*, 39, 235-259, 2001.

8 Kroll, J. H., Donahue, N. M., Jimenez, J. L., Kessler, S. H., Canagaratna, M. R., Wilson,
9 K. R., Altieri, K. E., Mazzoleni, L. R., Wozniak, A. S., Bluhm, H., Mysak, E. R., Smith,
10 J. D., Kolb, C. E., and Worsnop, D. R.: Carbon Oxidation State as a Metric for
11 Describing the Chemistry of Atmospheric Organic Aerosol, *Nature Chemistry*, 3, 133-
12 139, 2011.

13 Lanz, V. A., Alfarra, M. R., Baltensperger, U., Buchmann, B., Hüglin, C., and Prévôt, A.
14 S. H.: Source apportionment of submicron organic aerosols at an urban site by factor
15 analytical modelling of aerosol mass spectra, *Atmos. Chem. Phys.*, 7, 1503–1522, 2007.

16 Lee, A. K. Y., Herckes, P., Leaitch, W. R., Macdonald, A. M., and Abbatt, J. P. D.:
17 Aqueous OH oxidation of ambient organic aerosol and cloud water organics: Formation
18 of highly oxidized products, *Geophys. Res. Lett.*, 38, L11805,
19 doi:10.1029/2011GL047439,2011.

20 Leone, S. R., Ahmed, M., and Wilson, K. R.: Chemical dynamics, molecular energetics,
21 and kinetics at the synchrotron, *Phys. Chem. Chem. Phys.*, 12, 6564-6578, 2010.

22 Lin, Y.-H., Zhang, Z., Docherty, K. S., Zhang, H., Budisulistiorini, S. H., Rubitschun, C.
23 L., Shaw, S. L., Knipping, E. M., Edgerton, E. S., and Kleindienst, T. E.: Isoprene
24 epoxydiols as precursors to secondary organic aerosol formation: acid-catalyzed reactive
25 uptake studies with authentic compounds, *Environ. Sci. Technol.*, 46, 250-258, 2012.

26 Lopez-Hilfiker, F. D., Mohr, C., Ehn, M., Rubach, F., Kleist, E., Wildt, J., Mentel, T. F.,
27 Lutz, A., Hallquist, M., and Worsnop, D.: A novel method for online analysis of gas and

1 particle composition: description and evaluation of a Filter Inlet for Gases and AEROSols
2 (FIGAERO), *Atmos. Meas. Tech.*, 7, 983-1001, 2014.

3 Mazzoleni, L. R., Ehrmann, B. M., Shen, X. H., Marshall, A. G., and Collett, J. L.:
4 Water-soluble atmospheric organic matter in fog: exact masses and chemical
5 formula identification by ultrahigh-resolution Fourier transform ion cyclotron
6 resonance mass spectrometry, *Environ. Sci. Technol.*, 44
7 3690–3697, 2010.

8

9 McLafferty, F. W., and Turecek, F.: *Interpretation of Mass Spectra*, 1993.

10

11 Mensah, A. A., Buchholz, A., Mentel, T. F., Tillmann, R., and Kiendler-Scharr, A.:
12 Aerosol mass spectrometric measurements of stable crystal hydrates of oxalates and
13 inferred relative ionization efficiency of water, *J. Aerosol Sci.*, 42, 11-19, 2011.

14 Moldoveanu, S.: *Pyrolysis of Organic Molecules: Applications to Health and*
15 *Environmental Issues*, Elsevier Science, 2009.

16 Mysak, E. R., Smith, J. D., Ashby, P. D., Newberg, J. T., Wilson, K. R., and Bluhm, H.:
17 Competitive reaction pathways for functionalization and volatilization in the
18 heterogeneous oxidation of coronene thin films by hydroxyl radicals and ozone, *Phys.*
19 *Chem. Chem. Phys.*, 13, 7554-7564, 2011.

20 Nakao, S., Tang, P., Tang, X., Clark, C. H., Seo, Li. Q., E. , Asa-Awuku, A., and Cocker
21 III, D.: Density and Elemental Ratios of Secondary Organic Aerosol: Application of a
22 Density Prediction Method., *Atmos. Environ.*, 68, 273-277, 2013.

23 Ng, N. L., Canagaratna, M. R., Jimenez, J. L., Zhang, Q., Ulbrich, I. M., and Worsnop,
24 D. R.: Real-time methods for estimating organic component mass concentrations from
25 aerosol mass spectrometer data, *Environ. Sci. Technol.*, 45, 910-916, 2010a.

26 Ng, N. L., Canagaratna, M. R., Zhang, Q., Jimenez, J. L., Tian, J., Ulbrich, I. M., Kroll, J.
27 H., Docherty, K. S., Chhabra, P. S., Bahreini, R., Murphy, S. M., Seinfeld, J. H.,
28 Hildebrandt, L., Donahue, N. M., Decarlo, P. F., Lanz, V. A., Prevot, A. S. H., Dinar, E.,

1 Rudich, Y., and Worsnop, D. R.: Organic aerosol components observed in northern
2 hemispheric datasets from aerosol mass spectrometry, *Atmos. Chem. Phys.*, 10, 4625-
3 4641, 2010b.

4 Ng, N. L., Canagaratna, M. R., Jimenez, J. L., Chhabra, P. S., Seinfeld, J. H., and
5 Worsnop, D. R.: Changes in organic aerosol composition with aging inferred from
6 aerosol mass spectra, *Atmos. Chem. Phys.*, 11, 6465-6474, 2011.

7 Nguyen, H. P., and Schug, K. A.: The advantages of ESI-MS detection in conjunction
8 with HILIC mode separations: Fundamentals and applications, *Journal of Separation*
9 *Science* 31, 1465–1480, 2008.

10 Northway, M. J., Jayne, J. T., Toohey, D. W., Canagaratna, M. R., Trimborn, A.,
11 Akiyama, K.-I., Shimojo, A., Jiménez, J. L., DeCarlo, P. F., Wilson, K. R., and
12 Worsnop, D. R.: Demonstration of a VUV lamp photoionization source for improved
13 organic speciation in an aerosol mass spectrometer, *Aerosol Sci. and Technol.*, 41, 829-
14 839, 2007.

15 O'Brien, R. J., Holmes, J. R., and Bockian, A. H.: Formation of photochemical aerosol
16 from hydrocarbons. Chemical reactivity and products, *Environ. Sci. Technol.*, 9, 568-576,
17 1975.

18 Polidori, A., Turpin, B. J., Davidson, C. I., Rodenburg, L. A., and Maimone, F.: Organic
19 PM 2.5: Fractionation by polarity, FTIR spectroscopy, and OM/OC ratio for the
20 Pittsburgh aerosol, *Aerosol Sci. Tech.*, 42, 233-246, 2008.

21 Pope, C. A., and Dockery, D. W.: Health effects of fine particulate air pollution: lines that
22 connect. , *J Air Waste Manag Assoc.* , 56, 709-742, 2006.

23 S. Fuzzi, S. Decesari, Facchini, M. C., E. Matta, and Mircea, M.: A simplified model of
24 the water soluble organic component of
25 atmospheric aerosols, *Geophys. Res. Lett.*, 28, 4079–4082, 2001.

26 Smith, J. D., J. H. Kroll, Cappa, C. D., Che, D. L., Liu, C.-L., Ahmed, M., Leone, S. R.,
27 Worsnop, D. R., and Wilson, K. R.: The heterogeneous reaction of hydroxyl radicals with

1 sub-micron squalane particles: A model system for understanding the oxidative aging of
2 ambient aerosols, *Atmos. Chem. Phys.*, 9, 3209-3222, 2009.

3 Sun, Y., Zhang, Q., MacDonald, A. M., Hayden, K., Li, S. M., Liggio, J., Liu, P. S. K.,
4 Anlauf, K. G., Leaitch, W. R., Cubison, M. J., Worsnop, D., Van Donkelaar, A., and
5 Martin, R. V.: Size-resolved Aerosol Chemistry on Whistler Mountain, Canada with a
6 High-Resolution Aerosol Mass Spectrometer during INTEX-B, *Atmos. Chem. Phys.*, 9,
7 3095-3111, 2009.

8 Surratt, J. D., Murphy, S. M., Kroll, J. H., Ng, N. L., Hildebrandt, L., Sorooshian, A.,
9 Szmigielski, R., Vermeylen, R., Maenhaut, W., Claeys, M., Flagan, R. C., and Seinfeld,
10 J. H.: Chemical Composition of Secondary Organic Aerosol Formed from the
11 Photooxidation of Isoprene, *The Journal of Physical Chemistry A*, 110, 9665-9690, 2006.
12

13 Takegawa, N., Miyakawa, T., Kawamura, K., and Kondo, Y.: Contribution of selected
14 dicarboxylic and oxocarboxylic acids in ambient aerosol to the m/z 44 signal of an
15 Aerodyne Aerosol Mass Spectrometer, *Aerosol Sci. Tech.*, 41, 418-437, 2007.

16 Turpin, B. J., and Lim, H.-J.: Species contributions to PM_{2.5} mass concentrations:
17 Revisiting common assumptions for estimating organic mass, *Aerosol Sci. Tech.*, 35,
18 602-610, 2001.

19 Ulbrich, I. M., Canagaratna, M. R., Zhang, Q., Worsnop, D. R., and Jimenez, J. L.:
20 Interpretation of Organic Components from Positive Matrix Factorization of Aerosol
21 Mass Spectrometric Data, *Atmos. Chem. Phys.*, 9, 2891-2918, 2009.

22 Williams, B., Goldstein, A., Kreisberg, N., and Hering, S.: An In-Situ Instrument for
23 Speciated Organic Composition of Atmospheric Aerosols: Thermal Desorption Aerosol
24 Gc/MS-FID (TAG), *Aerosol Sci. and Technol.*, 40, 627-638, 2006.

25 Williams, B. J., Jayne, J. T., Lambe, A. T., Hohaus, T., Kimmel, J. R., Sueper, D.,
26 Brooks, W., Williams, L. R., Trimborn, A. M., Hayes, P. L., Jimenez, J. L., Kreisberg, N.
27 M., Hering, S. V., Worton, D. R., Goldstein, A. H., and Worsnop, D. R.: The First
28 Combined Thermal Desorption Aerosol Gas Chromatograph - Aerosol Mass

1 Spectrometer (TAG-AMS), *Aerosol Sci. Tech.*, 48, 358-370,
2 doi:10.1080/02786826.2013.875114, 2014.

3

4 Yatavelli, R. L. N., and Thornton, J. A.: Particulate organic matter detection using a
5 micro-orifice volatilization impactor coupled to a chemical ionization mass spectrometer
6 (MOVI-CIMS), *Aerosol Sci. and Technol.*, 44, 61-74, 2010.

7 Zhang, Q., Alfarra, M. R., Worsnop, D. R., Allan, J. D., Coe, H., Canagaratna, M. R., and
8 Jiménez, J. L.: Deconvolution and quantification of hydrocarbon-like and oxygenated
9 organic aerosols based on aerosol mass spectrometry, *Environ. Sci. and Technol.*, 39,
10 4938-4952 doi:4910.1021/es048568l, 2005.

11 Zhang, Q., Jimenez, J., Canagaratna, M., Ulbrich, I., Ng, N., Worsnop, D., and Sun, Y.:
12 Understanding atmospheric organic aerosols via factor analysis of aerosol mass
13 spectrometry: a review, *Anal. Bioanal. Chem.*, 401, 3045-3067, 2011.

14 Zhang, Z., Lin, Y.-H., Zhang, H., Surratt, J. D., Ball, L. M., and Gold., A.: Technical
15 Note: Synthesis of isoprene atmospheric oxidation products: isomeric epoxydiols and
16 the rearrangement products cis- and trans-3-methyl-3,4-dihydroxytetrahydrofuran,
17 *Atmopheric Chemistry and Physics*, 12, 8529-8535, 2012.

18
19
20

1 Table 1. A list of standards analyzed in this study and their molecular O:C and H:C
 2 ratios. Standards are categorized according to their functionality into broad groups. All
 3 standards were studied with EI AMS, while standards also studied with VUV-AMS are
 4 noted in the last column.

	Name	Formula	O:C	H:C	VUV-AMS
Multifunctional	Cis-Pinonic Acid	C ₁₀ H ₁₄ O ₃	0.3	1.4	X
	2-Oxooctanoic Acid	C ₈ H ₁₄ O ₃	0.37	1.75	
	Acetylsalicylic Acid	C ₉ H ₈ O ₄	0.44	0.89	X
	Homovanillic Acid	C ₉ H ₁₀ O ₄	0.44	1.11	X
	4-Acetylbutyric Acid	C ₆ H ₁₀ O ₃	0.5	1.67	
	5-Oxoazaleic Acid	C ₉ H ₁₄ O ₅	0.55	1.56	X
	Levulinic Acid	C ₅ H ₈ O ₃	0.6	1.6	
	Gamma Ketopimelic Acid	C ₇ H ₁₀ O ₅	0.71	1.43	X
	3-Hydroxybutyric Acid	C ₄ H ₈ O ₃	0.75	2	
	2-Ketobutyric Acid	C ₄ H ₆ O ₃	0.75	1.5	
	3-Hydroxy-3-Methylglutaric Acid	C ₆ H ₁₀ O ₅	0.83	1.67	
	1,3-Acetonedicarboxylic Acid	C ₅ H ₆ O ₅	1	1.2	
	□-Ketoglutaric Acid	C ₅ H ₆ O ₅	1	1.2	X
	Lactic Acid	C ₃ H ₆ O ₃	1	1.67	
	Pyruvic Acid	C ₃ H ₄ O ₃	1	1.33	
	Citric Acid	C ₆ H ₈ O ₇	1.16	1.33	X
	Diglycolic Acid	C ₄ H ₆ O ₅	1.25	1.5	
	Malic Acid	C ₄ H ₆ O ₅	1.25	1.5	X
	Oxaloacetic Acid	C ₄ H ₄ O ₅	1.25	1	
	Glycolic Acid	C ₂ H ₄ O ₃	1.5	2	
Tartaric Acid	C ₄ H ₆ O ₆	1.5	1.5	X	
Alcohols	<i>Cis</i> -3-methyl-3,4-dihydroxytetrahydrofuran	C ₅ H ₁₀ O ₃	0.6	2	
	Racemic mixture of □-Isoprene Epoxydiols	C ₅ H ₁₀ O ₃	0.6	2	
	<i>Trans</i> -3-methyl-3,4-dihydroxytetrahydrofuran	C ₅ H ₁₀ O ₃	0.6	2	
	Mannitol	C ₆ H ₁₄ O ₆	1	2.33	
	Mannose	C ₆ H ₁₂ O ₆	1	2	X
	Sucrose	C ₁₁ H ₂₃ O ₁₁	1	2.09	X
	Xylitol	C ₅ H ₁₂ O ₅	1	2.4	X
Diacids	Sebacic Acid	C ₁₀ H ₁₈ O ₄	0.4	1.8	
	Azalaic Acid	C ₉ H ₁₆ O ₄	0.44	1.78	
	Pimelic Acid	C ₇ H ₁₂ O ₄	0.57	1.71	X
	Adipic Acid	C ₆ H ₁₀ O ₄	0.66	1.67	X
	Glutaric Acid	C ₅ H ₈ O ₄	0.8	1.6	X
	Malaic Acid	C ₄ H ₄ O ₄	1	1	X
	Succinic Acid	C ₄ H ₆ O ₄	1	1.5	X
	Malonic Acid	C ₃ H ₄ O ₄	1.33	1.33	X
	Oxalic Acid	C ₂ H ₂ O ₄	2	1	
Polyacids	1,3,5-Cyclohexanetricarboxylic Acid	C ₆ H ₉ O ₆	1	1.5	X
	Tricarballic Acid	C ₆ H ₈ O ₆	1	1.33	X
	1,2,4,5-Benzenetetracarboxylic Acid	C ₆ H ₆ O ₈	1.33	1	X
Esters	Dibutyl Oxalate	C ₈ H ₁₈ O ₄	0.5	2.25	
	Gamma Ketopimelic Acid Dilactone	C ₆ H ₈ O ₄	0.57	1.14	X
	Ethyl Pyruvate	C ₅ H ₈ O ₃	0.6	1.6	
	Dimethyl 1,3-Acetonedicarboxylate	C ₇ H ₁₀ O ₅	0.71	1.43	

1 Table 2: Summary of fragment ion ratios observed for standard molecules, chamber
 2 SOA, and ambient SOA. The entry * denotes the use of Aiken assumptions for the ratio in
 3 the frag Table.
 4

	Obs H_2O^+/CO_2^+	Obs CO^+/CO_2^+	Frag Wave H_2O^+/CO_2^+ RIE H2O=1.4	Frag Wave H_2O^+/CO_2^+ RIE H2O=2	Literature Reference
AMS Frag Table					
Aiken Assumptions	0.32	1	0.32	0.225	Aiken et al.(2008)
OA Standards					
Multifunctional	0.5-1.5	1-2	0.5-1.5	0.35-1.05	This Study
Polyacids	1	1-2	1	0.7	
Diacids	2	2	2	1.4	
Esters	0.5-1	1	0.5-1	0.35-0.7	
Alcohols	>10	>4	>10	>7	
Ambient Aerosol					
Pittsburgh, USA	*	1.3	*	*	Zhang et al.(2005)
Tokyo, Japan	*	1	*	*	Takegawa et al. (2007)
Whistler Mtn, Canada	1	*	1	0.7	Sun et al.,(2009)
Chamber SOA					
Isoprene Photooxidation (Low NOx)	3.9	1.03-2.6	3.9	2.7	Chhabra et al. (2010); Chen et al.(2011)
Isoprene Photooxidation (NOx)	0.3	*	0.3	0.2	Nakao et al., (2013)
-pinene+O3	0.8-1	1-1.1	0.8-1	0.6-0.7	Chhabra et al.(2010), Chen et al. (2011),Nakao et al. (2013)
-caryophyllene+O3	0.7-1.3	1.2	0.7-1.3	0.5-0.9	Chen et al.(2011), Nakao et al.(2013)
Toluene Photooxidation (NOx)	1.8	1	1.8	1.3	Hildebrandt et al.,(2014)
Aromatics Photooxidation (NOx, Low NOx)	0.3-1.3	*	0.3-1.3	0.2-0.9	Nakao et al.(2013)
Naphthalene Photooxidation (Low NOx)	*	1.2	*	*	Chhabra et al.(2011)

5

1 **Table 3.** Summary of elemental composition information obtained for chamber and
 2 ambient OA.

3

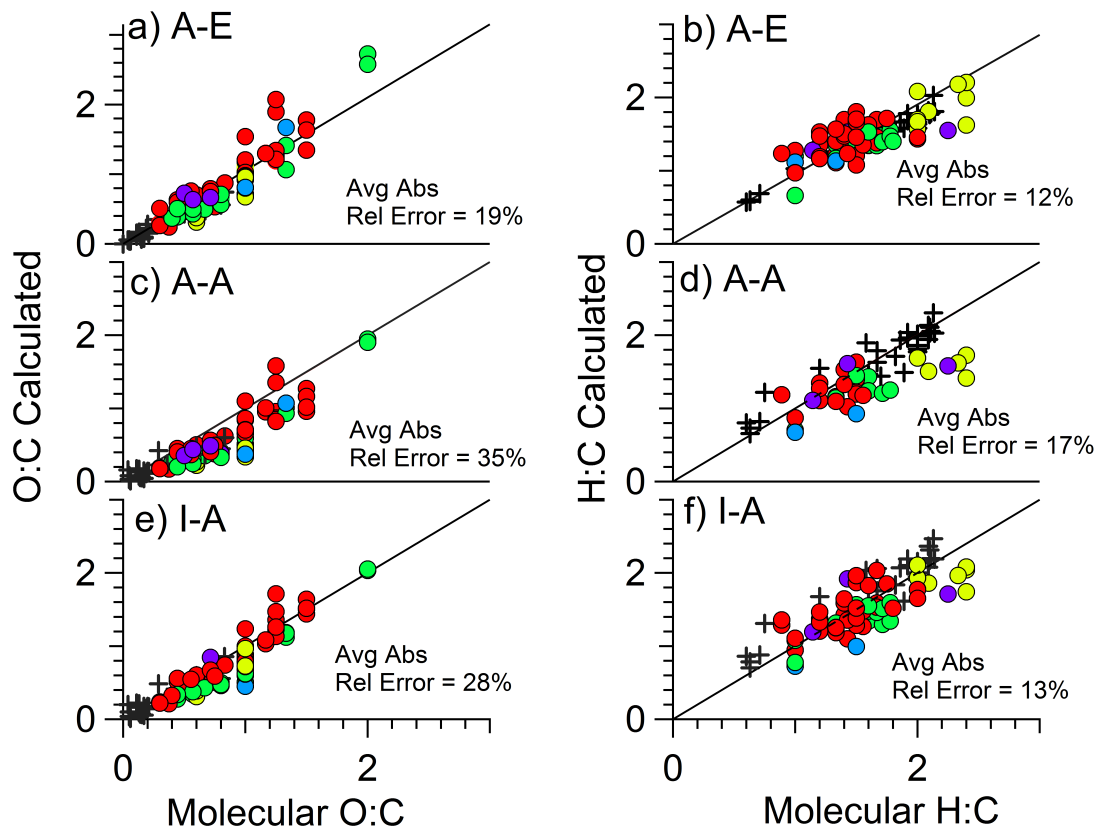
	Improved-Ambient				Change (with respect to Aiken-Ambient)				Literature Reference
	O:C	H:C	OM:OC	Osc	O:C (%)	H:C (%)	OM:OC (%)	Osc (Absolute)	
Ambient OA									See Table S1 for full list
Total OA	0.52	1.65	1.84	-0.60	27	11	9	0.06	
<i>Primary Components</i>									
HOA	0.13	1.96	1.34	-1.69	27	8	4	-0.09	
BBOA	0.36	1.76	1.64	-1.04	34	11	9	0.01	
COA	0.22	1.81	1.45	-1.37	32	11	6	-0.06	
<i>Secondary Components</i>									
SV-OOA	0.53	1.62	1.84	-0.57	32	12	11	0.07	
LV-OOA	0.84	1.43	2.25	0.25	25	12	12	0.19	
Total OOA	0.67	1.54	2.03	-0.19	28	12	11	0.13	
Chamber SOA									
Isoprene	0.87	1.94	2.33	-0.19	57	23	24	0.27	Chen et al. (2011)
α -pinene	0.41	1.48	1.67	-0.65	24	9	7	0.04	Chen et al. (2011)
β -caryophyllene	0.47	1.52	1.75	-0.58	29	11	10	0.06	Chen et al. (2011)
Toluene	0.85	1.67	2.28	0.10	50	25	22	0.30	Hildebrandt Ruiz et al. (2014)

4

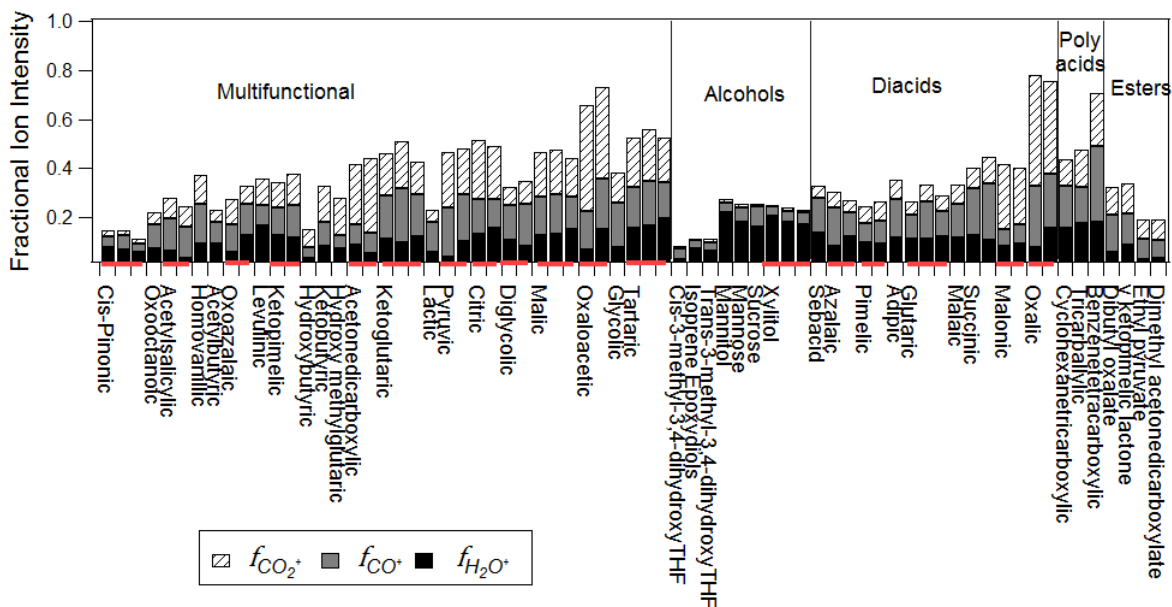
5

6

● Multifunctional, Esters, Polyacids, Alcohols, Diacids;
+ Aiken(2007,2008)



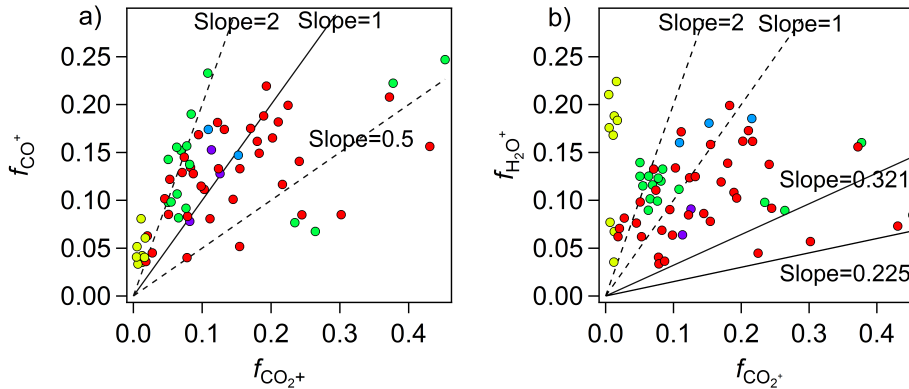
1
2 Figure 1: Scatter plots between known elemental compositions and AMS elemental ratios
3 obtained with the Aiken-Explicit (A-E; panels a and b), Aiken-Ambient (A-A; panels c
4 and d), and Improved-Ambient methods (I-A; panels e and f). A 1:1 line is shown for
5 reference in all plots. The standards examined in this study are colored according to their
6 chemical functionality. Also shown are previously published standard molecule data
7 from Aiken et al. (2007).



1 Figure 2: Fractional AMS ion intensities (relative to the total ion signal for each standard)
 2 measured for CO_2^+ , CO^+ , and H_2O^+ from each of the laboratory aerosol standards studied
 3 here. The standards are classified according to functionality and then arranged according
 4 to increasing O:C. Repeat measurements were performed for some of the standards to
 5 investigate the consistency of measured mass spectra between different HR-ToF-AMS
 6 instruments. Repeat measurements performed for the same standard are arranged
 7 together and denoted by red horizontal bars on the bottom axis of the graph.

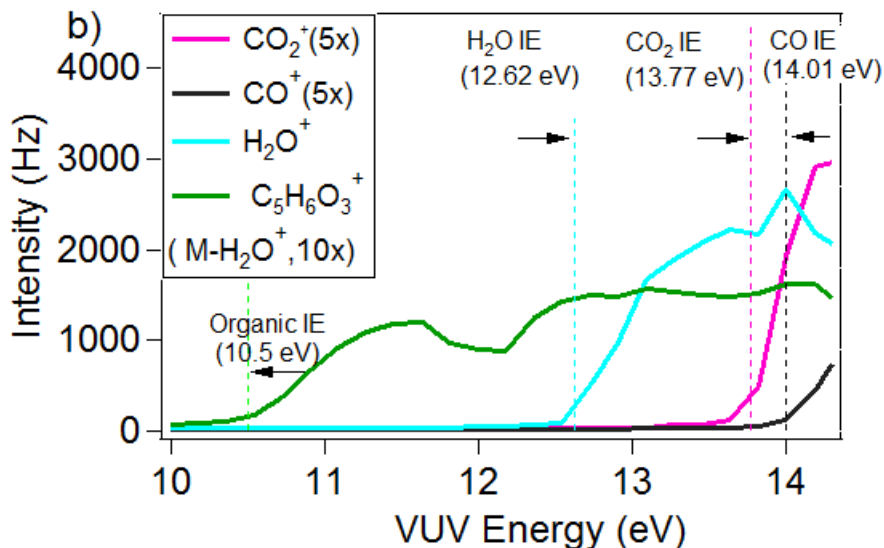
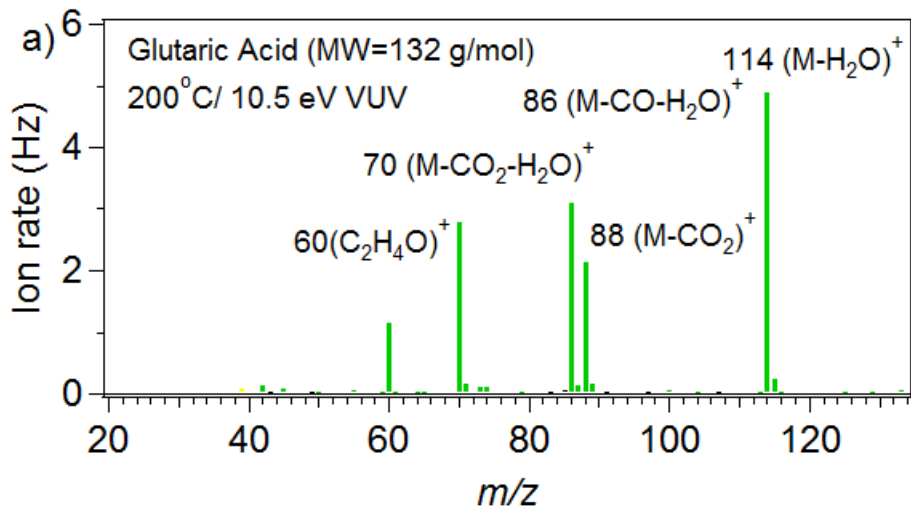
8
 9
 10
 11
 12
 13
 14
 15
 16
 17

Standards
 Multifunctional, Esters, Polyacids, Alcohols, Diacids



1
2
3
4
5
6
7
8
9

Figure 3: Scatter plots between AMS fractional ion intensities for CO^+ and CO_2^+ (panel a) and H_2O^+ and CO_2^+ (panel b). The empirical ratios used for each of these relationships in the Aiken-Ambient calculations are shown as solid lines with the appropriate slopes. In panel (b) two solid lines are shown to reflect the measured ratios that correspond to possible H_2O RIE values ranging from 1.4 to 2 (See Sect. 2 for more information). Dashed lines on both panels are included for reference to visualize the range of slope values.

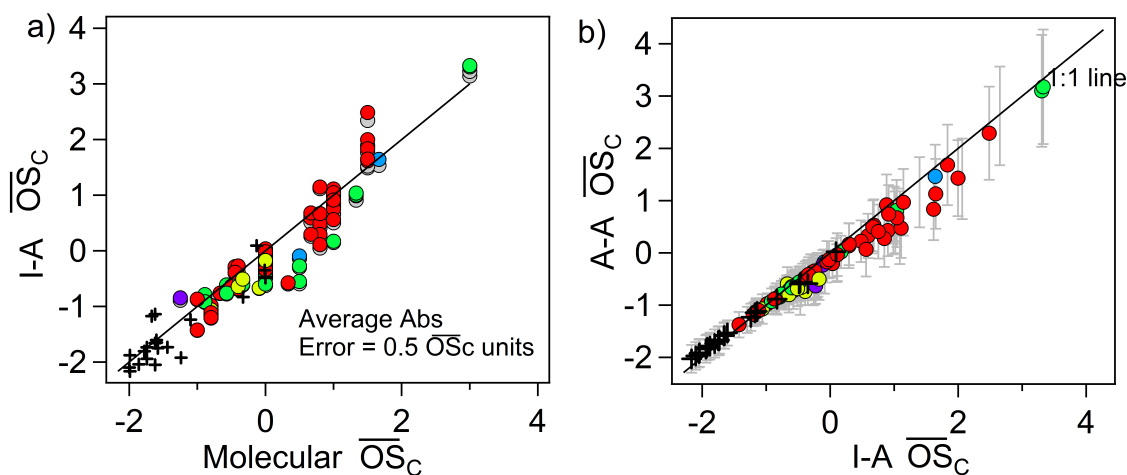


1
 2 Figure 4: a) VUV-AMS spectrum of glutaric acid obtained under an argon atmosphere.
 3 The spectrum was obtained at a VUV energy of 10.5 eV and a vaporizer temperature of
 4 200°C. Ions corresponding to loss of CO₂, CO, and H₂O moieties from the parent ion
 5 (M⁺) are observed. b) Glutaric acid VUV-AMS signals as a function of VUV
 6 monochromatic photon energy. The signal intensity of C₅H₆O₃⁺ which corresponds to
 7 the [M-H₂O]⁺ ion, and the signal intensities of CO₂⁺, CO⁺, H₂O⁺ are shown. The gas
 8 phase ionization energies (IE) for neutral CO₂, CO, and H₂O molecules are shown as
 9 colored vertical lines.

10

1

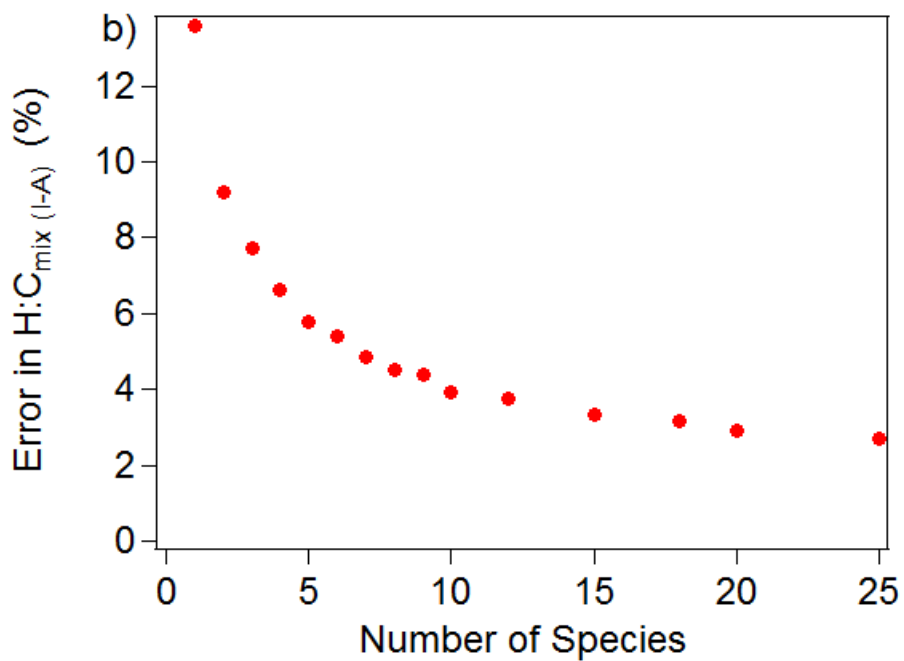
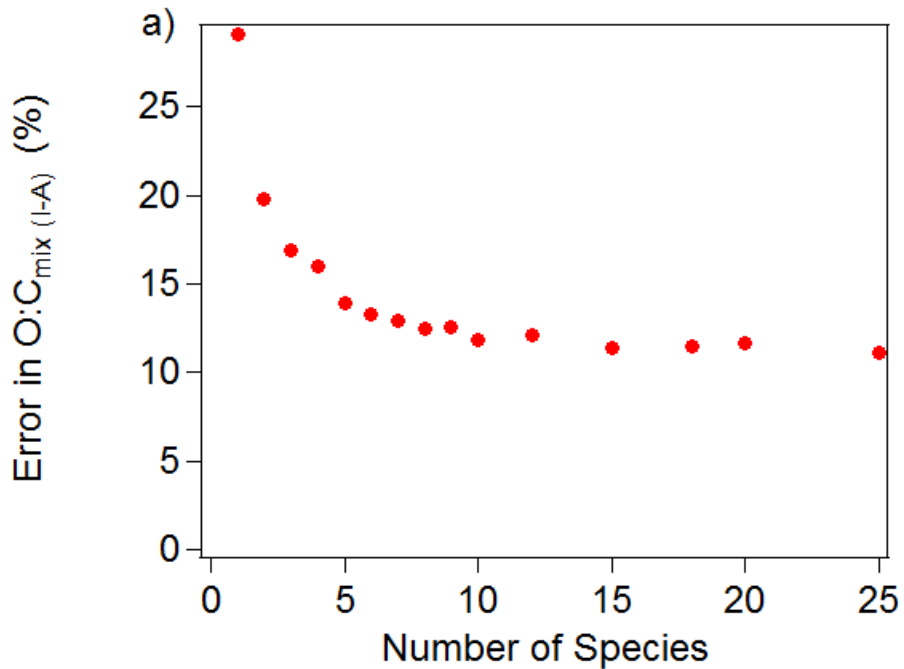
- Default Frag Wave
Multifunctional, Esters, Polyacids, Alcohols, Diacids
- Hildebrandt Frag Wave
- + Aiken et al. (2007,2008)



2

3 Figure 5: a) Scatter plot of Improved-Ambient \overline{OS}_C values ($2 \times O:C - H:C$) of the
4 organic standards vs. their known molecular \overline{OS}_C values. The Improved-Ambient
5 method was applied with the default AMS organic fragmentation wave (colored solid
6 circles) as well as with the Hildebrandt Ruiz et al. (2014) changes to the organic
7 fragmentation wave. b) Scatter plot of Aiken-Ambient \overline{OS}_C values of the organic
8 standards vs. the corresponding Improved-Ambient method values. The error bars
9 denote the propagated uncertainty in the Aiken-Ambient \overline{OS}_C values due to the
10 uncertainties in the Aiken-Ambient O:C and H:C values. The solid line shows the 1:1
11 relationship.

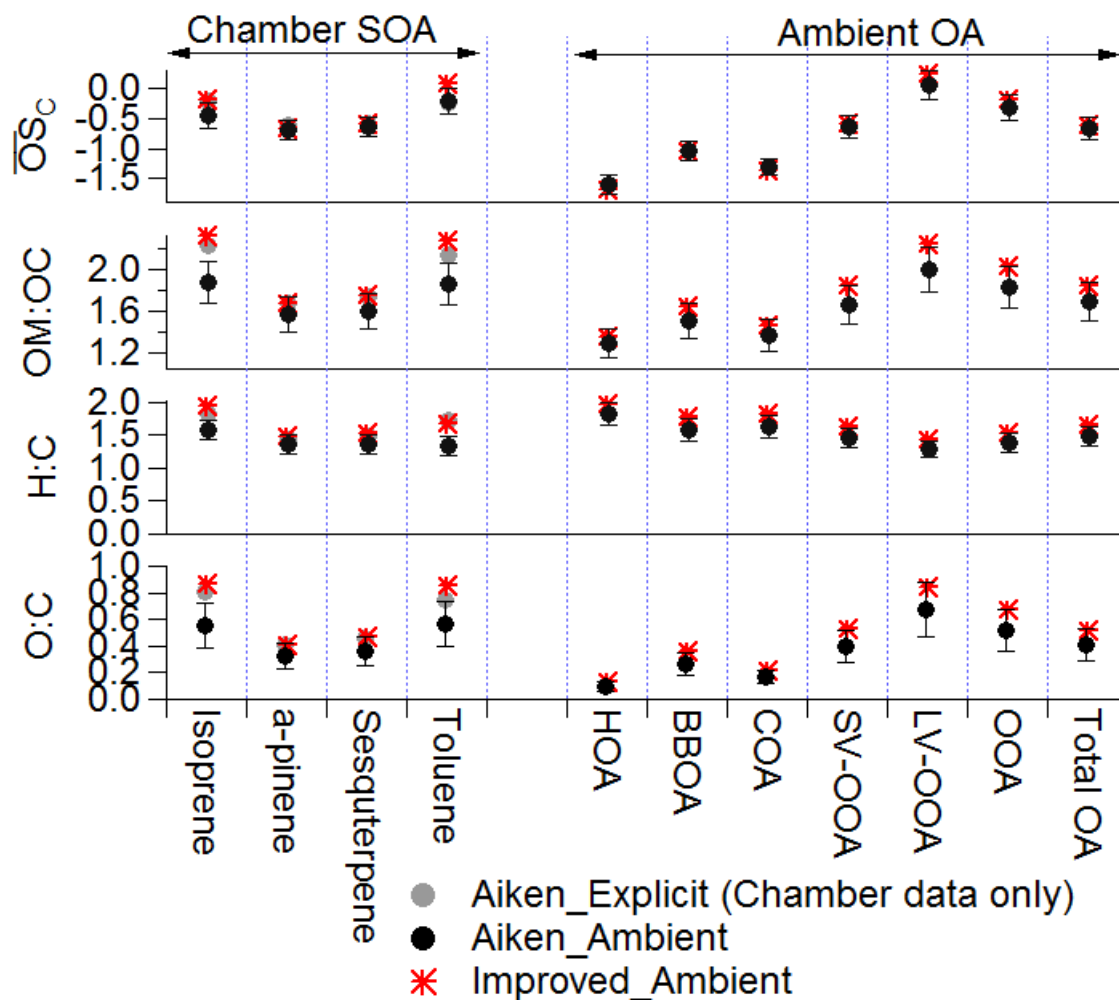
1



2

3 Figure 6: a) Errors in Improved-Ambient O:C ratio of organic standard molecule
4 mixtures as a function of number of species in the mixture. b) Errors in Improved-
5 Ambient H:C ratio of the organic standard molecule mixtures as a function of number of
6 species in the mixture.

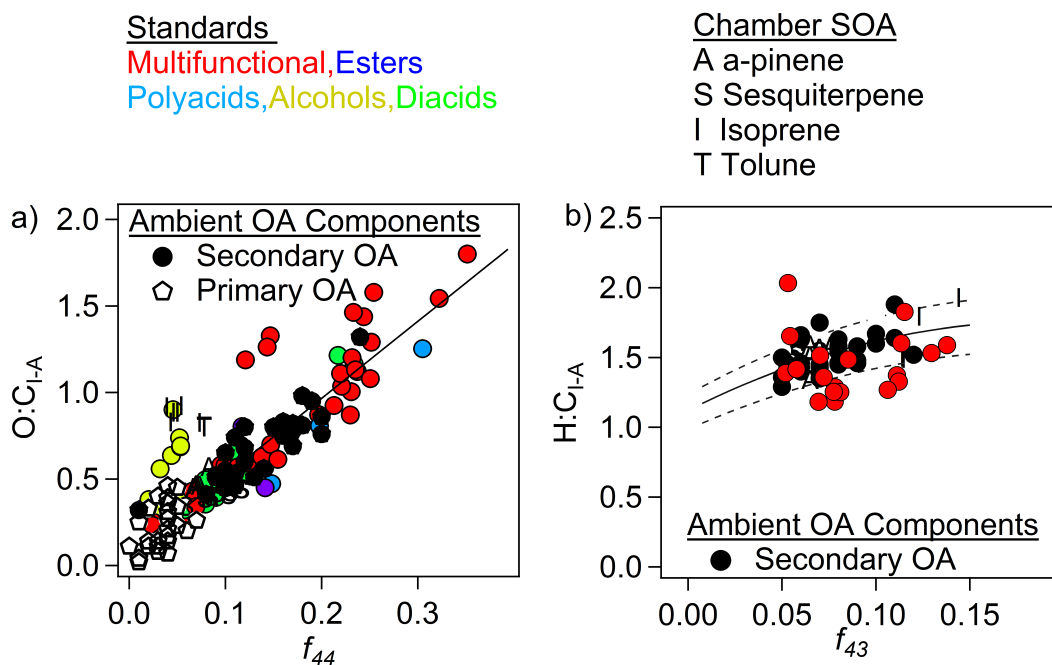
7



1 Figure 7: Summary of elemental composition information obtained across chamber and
 2 ambient OA measurements. The figure shows values obtained with the Improved-
 3 Ambient method as well as the Aiken-Ambient method. Aiken-Ambient elemental ratios
 4 are shown with errors from Aiken et al. (2007,2008) for reference. For the chamber
 5 data, Aiken-Explicit values measured by Chen et al. (2011) and Hildebrandt Ruiz et al.
 6 (2014) are also shown.

7
 8
 9
 10
 11

1



2

3 Figure 8: Scatter plot between Improved-Ambient O:C values and f_{44} (fractional ion
4 intensity at m/z 44 from unit mass resolution data). Ambient OA component data from
5 field campaigns are shown as black points. The black line shows the linear fit through
6 the ambient OA ($O:C_{I-A} = 0.079 + 4.31 \times f_{44}$). Chamber SOA and standard OA data are
7 also shown in the figure. b) Scatter plot between Improved-Ambient H:C values and f_{43}
8 for ambient secondary OA components and chamber SOA. OA standard data is shown
9 for the few multifunctional species which fit the criteria for this parameterization ($f_{44} >$
10 0.05 and $f_{43} > 0.04$). The solid line shows a scaled version of the Ng et al.
11 parameterization ($H:C_{\text{Improved Ambient}} = 1.12 + 6.74 \times f_{43} + 17.77 \times f_{43}^2$) and the dotted lines
12 show $\pm 10\%$ deviations from the parameterization.

13

14

15

16

17

18

19